From DEPARTMENT OF CLINICAL NEUROSCIENCE
Karolinska Institutet, Stockholm, Sweden

A STUDY OF THE FOVEAL STRUCTURE IN PREMATURELY BORN CHILDREN BY THE USE OF OPTICAL COHERENCE TOMOGRAPHY

Rebecka Rosén

Karolinska Institutet

Stockholm 2018

Published by Karolinska Institutet.
Printed by Eprint AB 2018

ISBN 978-91-7676-924-9

A STUDY OF THE FOVEAL STRUCTURE IN PREMATURELY BORN CHILDREN BY THE USE OF OPTICAL COHERENCE TOMOGRAPHY
THESIS FOR DOCTORAL DEGREE (Ph.D.)

AKADEMISK AVHANDLING
som för avläggande av medicine doktorsexamen vid Karolinska Institutet offentligen försvaras i Widmarksalen, S:t Eriks Ögonsjukhus.

Fredagen 21 september 2018, kl 13

By

Rebecka Rosén

Principal Supervisor:
Senior Lecturer Maria Nilsson
Karolinska Institutet
Department of Clinical Neuroscience
Division of Eye and Vision
Unit of Optometry

Co-supervisor(s):
Professor Lene Martin
Mälardalens Högskola
School of health, care and social welfare

Associate Professor Kerstin Hellgren
Karolinska Institutet
Department of Clinical Neuroscience

Opponent:
Professor Sten Andréasson
Lunds universitet
Department of Clinical Sciences
Division of Ophthalmology

Examination Board:
Associate Professor Linda Lundström
Kungliga tekniska högskolan
Department of Applied Physics

Associate Professor Stefan Löfgren
Karolinska Institutet
Department of Clinical Neuroscience

Professor Olav Haugen
Universtitetet i Bergen
Department of Clinical Medicine

To my dear family

ABSTRACT

During the last decades there has been a rapid development in techniques for retinal imaging. The optical coherence tomography (OCT) examination is non-invasive, fast and patient-friendly which are good qualities when examining children. There is a steadily increasing survival rate of extremely premature infants due to improved neonatal care. These children are at higher risk of having visual impairment and OCT gives important information about the retinal structure in these children.

Purpose: The purpose of the first study was to evaluate different methods for examination and evaluation of the retinal structure. The purpose of study II, III and IV was to investigate and describe the foveal anatomy in 6.5 year old children born extremely preterm (EPT) by comparing the immature fovea and the normally developed fovea in age-matched control children.

Methods: The macular thickness was measured in healthy adult subjects and patients with macular oedema with the Heidelberg Retina Tomograph 3 (HRT3) and the Stratus OCT (study I). The study cohort in study II, III and IV were children born EPT and age-matched control children from Stockholm health care region (study II and IV) and from Stockholm and Uppsala health care region (study III). All participants were from the national population based Extremely Preterm Infants in Sweden Study (EXPRESS), which investigates the short- and long-term morbidity and mortality in infants born before 27 weeks of gestational age (GA). At the age of 6.5 years the children had their macular structure imaged with Cirrus SD-OCT. In study II and IV the foveal structure were evaluated by measuring foveal depth (FD), inner retinal layer (IRL), ganglion cell layer (GCL) and inner plexiform layer (IPL) (GCL+ when combined), outer nuclear layer (ONL) and outer segment (OS) thickness. In study III macular thickness was measured in 9 areas defined by the Early Treatment Diabetic Retinopathy Study as the ETDRS grid.

Results: In study I, no significant differences were found between the measurements at different sessions for any of the imaging techniques in either patients (n=9) or healthy subjects (n=30). The HRT3 showed lower repeatability and reproducibility compared to Stratus OCT. The results from study II, showed that children born EPT (n=30) had a shallower FD, thicker IRL and thicker ONL at the foveal center comped to children born at term (n=10). In study III, the 134 children born EPT had significantly thicker central macula compared to the 145 control children. Study IV showed that the 89 children born EPT has thicker central GCL+ thickness and reduced FD compared to the 92 children born at term. Low GA, retinopathy of prematurity (ROP), and male sex within the EPT group were associated with a thicker central macula in study III and reduced FD and increased central GCL+ thickness in study IV. In study IV, ROP treatment was also an associated factor.

Conclusion: The measurements with the HRT3 had lower repeatability and reproducibility compared with the Stratus OCT and OCT came out as a more promising technique for examination of children. Macular imaging using OCT has shown that a preterm birth can

inhibit foveal maturation resulting in structural deviations. Typical signs are a shallow FD, thicker IRL and GCL+ at the foveal center, contributing to a thicker central macular thickness. Low GA, ROP, ROP treatment and male sex are factors associated to these structural deviations.

LIST OF SCIENTIFIC PAPERS

I. **Rosén, R.**, Nilsson, M., Tallstedt, L., Martin, L.(2012). Test-retest variation in macular thickness measurements with the Heidelberg Retina Tomograph. *Clin Exp Opto, 95*(5), 515-521.
II. **Rosén, R.**, Sjöstrand, J., Nilsson, M., Hellgren, K. (2015). A methodological approach for evaluation of foveal immaturity after extremely preterm birth. *Ophthalmic Physiol Opt, 35*(4), 433-441.
III. Molnar, A. E., **Rosén, R. M.**, Nilsson, M., Larsson, E. K., Holmström, G. E., Hellgren, K. M. (2017). Central macular thickness in 6.5-year-old children born extremely preterm is strongly associated with gestational age even when adjusted for risk factors. *Retina, 37*(12), 2281-2288.
IV. **Rosén, R.**, Hellgren, K., Venkataraman, A., Dominguez Vicent, A., Nilsson, M. Increased foveal ganglion cell- and inner plexiform layer thickness in children aged 6.5 years born extremely preterm. *Submitted*

LIST OF ADDITIONAL SCIENTIFIC PAPERS

I. Brautaset, R., Birkeldh, U., **Rosén, R.**, Ramsay, M. W., & Nilsson, M. (2014). Reproducibility of disc and macula optical coherence tomography using the Canon OCT-HS100 as compared with the Zeiss Cirrus HD-OCT. *Eur J Ophthalmol, 24*(5), 722-727.
II. Brautaset, R. L., **Rosén, R.**, Cerviño, A., Miller, W. L., Bergmanson, J., & Nilsson, M. (2015). Comparison of Macular Thickness in Patients with Keratoconus and Control Subjects Using the Cirrus HD-OCT. *Biomed Res Int*, 2015;2015:832863.
III. Sjöstrand, J., **Rosén, R.**, Nilsson, M., & Popovic, Z. (2017). Arrested Foveal Development in Preterm Eyes: Thickening of the Outer Nuclear Layer and Structural Redistribution Within the Fovea. *Invest Ophthalmol Vis Sci, 58*(12), 4948-4958.

CONTENTS

LIST OF ABBREVIATIONS

BW	Birth weight
ETDRS	Early Treatment Diabetic Retinopathy Study
EXPRESS	Extremely Preterm Infants in Sweden Study
EPT	Extremely preterm
ELM	External limiting membrane
FW	Foetal week
FD	Foveal depth
FAZ	Foveal avascular zone
GA	Gestational age
GCL	Ganglion cell layer
HFL	Henle fiber layer
HRT	Heidelberg Retina Tomography
ILM	Inner limiting membrane
INL	Inner nuclear layer
IPL	Inner plexiform layer
IRL	Inner retinal layers
IS	Inner segment
IVH	Intraventricular haemorrhage
LGN	Lateral geniculate nucleus
NFL	Nerve fiber layer
n	Number
OCT	Optical coherence tomography
ONL	Outer nuclear layer
OPL	Outer plexiform layer
OS	Outer segment
RPE	Retinal pigment epithelium
ROP	Retinopathy of prematurity
SD	Spectral domain
SD	Standard deviation
SE	Spherical equivalent

TD	Time domain
VA	Visual acuity
VEGF	Vascular endothelial growth factor
µm	Micrometer

1 INTRODUCTION

Retinal imaging has revolutionized eye health care and provided new information about the retinal structure *in vivo* during recent years. In 1991 the Optical Coherence Tomography (OCT) technique was described for the first time (Huang et al., 1991), which allows highly repeatable measurements and 3-dimensional (3D) anatomical viewing of the retinal structure with high resolution. The OCT image can be seen as a "virtual biopsy" and studies have showed high correlation between OCT images and histological samples (Dubis et al., 2012; Vajzovic et al., 2012). The possibility to investigate retinal structures non-invasively and in real time has provided new information regarding both the normal retinal anatomy and how it is affected in different pathological conditions (Fujimoto & Swanson, 2016). Children born preterm constitute a specific group of patients, in which the normal retinal maturation can be inhibited and the risk of retinal pathology is increased.

The Extremely Preterm Infants in Sweden Study (EXPRESS) is a national and population based study with the aim of investigating short- and long-term morbidity and mortality in infants born before 27 weeks of gestational age (GA) in Sweden (Fellman et al., 2009). These children are predisposed to have reduced visual function and retinal development. The recent developments in the retinal imaging techniques have made it possible to describe the foveal structure in preterm children which was the purpose of study II, III and IV.

The aim of this thesis was two-fold. First, to evaluate different methods for examination and evaluation of the retinal structure. Secondly, to investigate and describe the foveal anatomy in children born extremely preterm which was accomplished by comparing the under developed fovea and the normally developed fovea.

2 BACKGROUND

2.1 THE HUMAN EYE

The human eye might be considered a small organ in size but is highly complicated in its structure. Although it is not actually the eye that sees, but the brain, it is the structure where the image is formed and the neural transmission and interpretation of light impulses begins. The eye is a three layer structure. The outer layer is composed of the cornea and the sclera. Next is the vascular layer, i.e. the uvea, made up of the choroid, ciliary body and iris. The lens is placed behind the iris. The inner most layer is the retina, a complex multi-layer structure with neurosensory properties. The space between the lens and the retina is filled up by the vitreous body, a transparent gel-like substance.

At birth, the axial length of the eye is around 17 mm and the eye continues to grow to around 24 mm into adulthood (Gordon, 1985). During childhood the radius of the cornea and lens elongates and their power reduces. The human eye is programmed to achieve emmetropia where the optical image is focussed on the retina and this emmetropisation is a result of two processes. The passive process is that the reduction of the power in the dioptric system needs to be proportional to the increasing axial length and the active process is the feedback from the retina about optical defocus and consequent adjustments of the axial length (Brown, Koretz, & Bron, 1999). If the emmetropisation process fails, it results in ametropia which means that the optical system of the eye does not match the axial length of the eye and the image is not correctly focused on the retina.

2.2 THE VISUAL PATHWAY

The retinotopic organization is very impressive, each retinal point projects to a specific area in the primary visual cortex, and there is a point-to-point representation of the visual field on the retina that is maintained through the visual pathways (Wärntges & Michelson, 2014). Rays of light pass through the cornea, lens, vitreous body and reach the retina. Light stimulates the photoreceptors and transforms into nerve impulses. These impulses are processed and transmitted by the inner retinal layers and then mediated through the ganglion cell axons towards the optic disc. The retinal ganglion cell axons form the optic nerve and pass the chiasm where the axons from the nasal retina in each eye cross over to join the temporal fibres from the fellow eye while the temporal axons continue uncrossed. The ganglion cells primarily project to the lateral geniculate nucleus (LGN) where they synapse with neurons. The axons of the LGN neurons pass through the optic radiation to the primary visual cortex where they synapse and connect to other parts of the brain (De Moraes, 2013), see Figure 1.

Figure 1. The visual pathways.

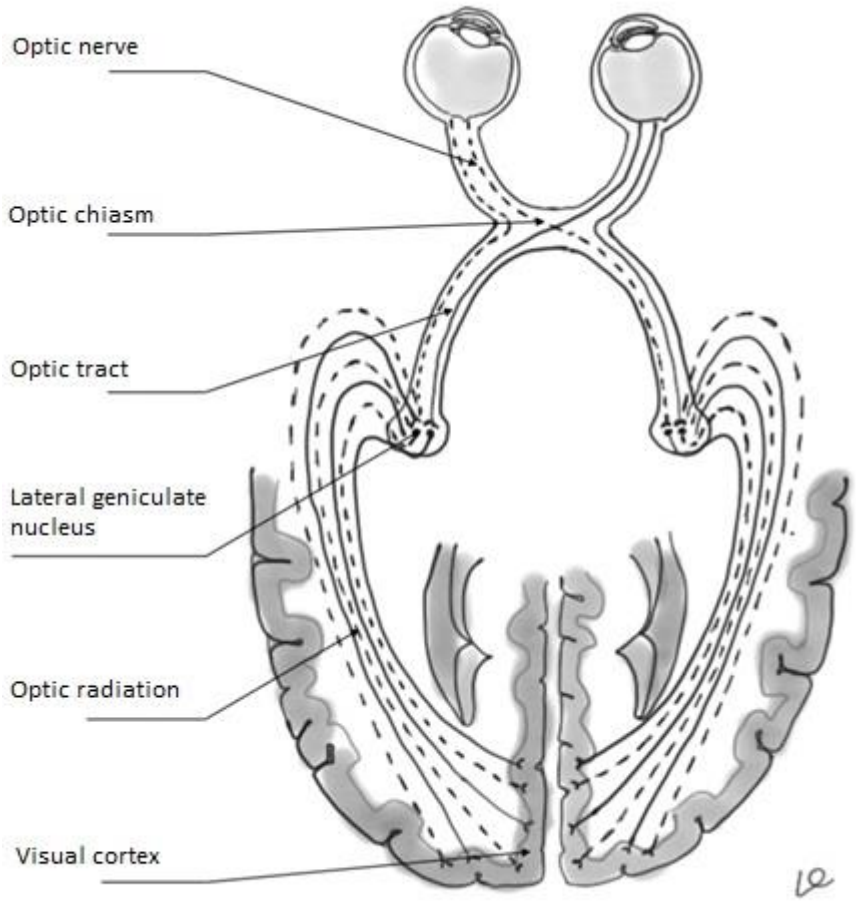

Illustration by L. Pettersson inspired from Hansen J. T. (2010). Netter's anatomy coloring book. (1st ed). Philadelphia: Saunders Elsevier.

The central vision is over represented in the visual cortex. The central 10° of the visual field occupies 50-60% of the surface area of the striate cortex (Horton & Hoyt, 1991; McFadzean, Brosnahan, Hadley, & Mutlukan, 1994).

2.3 THE NEURO RETINAL STRUCTURE

The retina is a part of the central nervous system together with the brain and the spinal cord. It is a thin transparent layer that consists of several cell layers and membranes. The inner retinal layers (IRL) include the inner limiting membrane (ILM), the nerve fibre layer (NFL), the ganglion cell layer (GCL), the inner plexiform layer (IPL) and the inner nuclear layer (INL). The outer retinal layers (ORL) include outer plexiform layer (OPL), the outer nuclear layer (ONL), the external limiting membrane (ELM), the photoreceptor layer with rods and cones and their inner and outer segments (IS and OS) and the retinal pigment epithelium (RPE), see Figure 2 and 4.

Figure 2. The retinal layers and cells.

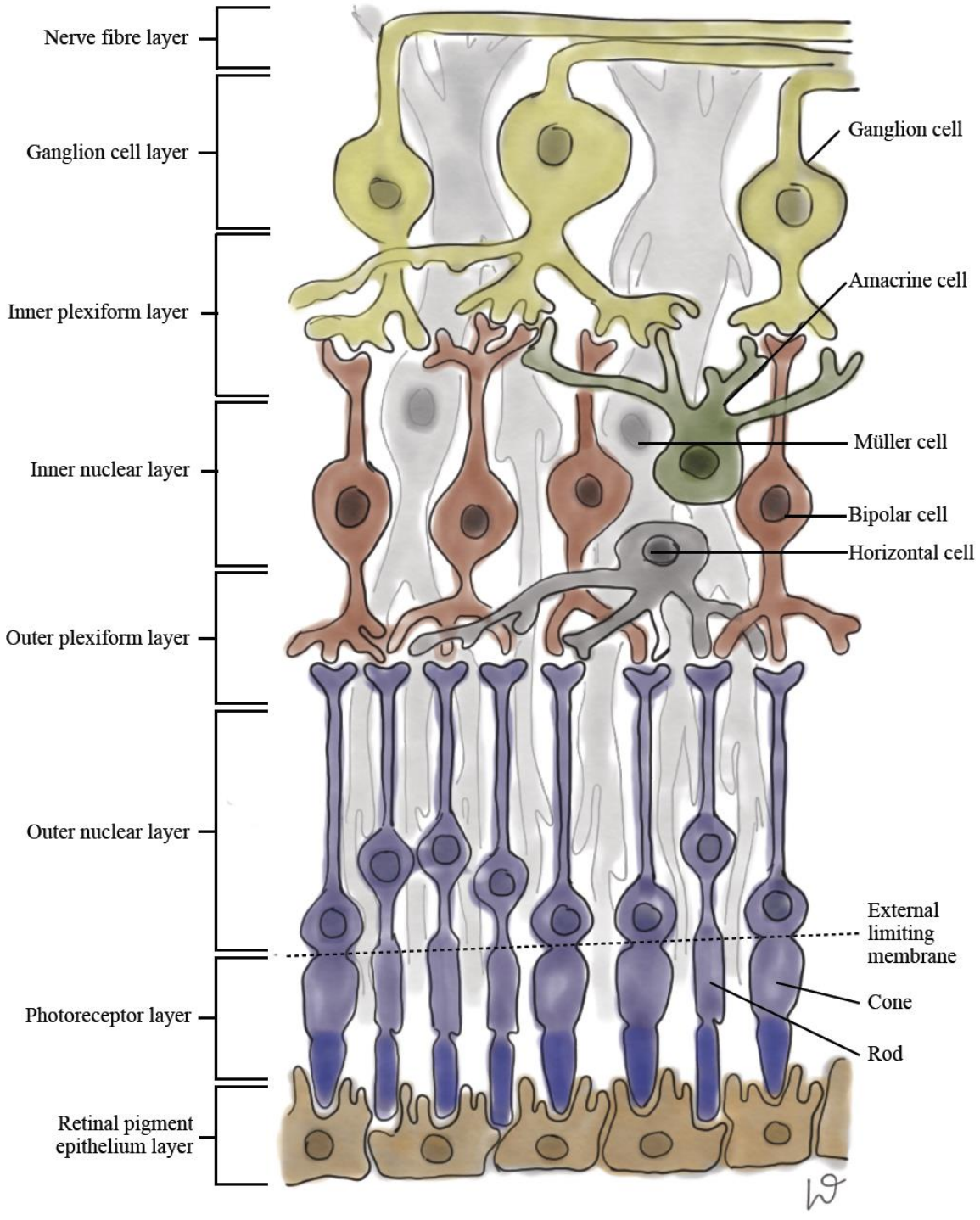

Illustration by L. Pettersson inspired from Hansen J. T. (2010). Netter's anatomy coloring book. (1st ed). Philadelphia: Saunders Elsevier.

2.3.1 The inner retinal layers

The ILM separates the retina from the vitreous body. The axons from the ganglion cells form the NFL and head towards the optic nerve. The GCL consist mainly of the nuclei of the ganglion cells but also displaced amacrine cells (Curcio & Allen, 1990). The number of ganglion cells varies highly between individuals and ranges between from 0.7 to 1.5 million. The ganglion cell density is around 32 000-38 000 cells/mm^2 in a horizontally elliptical ring around the FC. The ganglion cell density of the peripheral nasal and superior retina is 300% and 60% higher compared to corresponding temporal and inferior eccentricities (Curcio & Allen, 1990). A lot of ganglion cells are lost caused by genetically programmed cell death during the development of the eye. At foetal week (FW) 16-17 the number of axons at the optic nerve is around three times higher (3.7 million) than in adulthood (1.1-1.3 million) (Provis, van Driel, Billson, & Russell, 1985). The ganglion cells receive visual information from the photoreceptors through the bipolar cells and connect to each other through amacrine cells. There are several types of ganglion cells, but midget cells are the most numerous in and around the foveal depression (Polyak, 1949). These cells are specialised to transmit chromatic and high resolution information via the parvocellular pathways in the LGN (Polyak, 1949; Kolb, 2007). The high resolution is enabled by the high density of photoreceptors and that they are allowed to send information through one to three midget cells. In the more peripheral parts of the retina multiple photoreceptors sends information through the same ganglion cell, most often a parasol cell specialised on contrast and motion perception (Kolb, 2007). Sjöstrand, Olsson, Popovic and Conradi (1999) estimated that the ganglion cell-cone ratio is about 3 at the foveal border, about 1 outside the foveal border and then declines towards the peripheral retina.

In the IPL, bipolar- and amacrine cells connect with the ganglion cells. The amacrine cells are interneurons and mediate visual information input from bipolar cells onto ganglion cells. The nuclei of the bipolar-, horizontal- amacrine- and Müller cells are found in the INL.

2.3.2 The outer retinal layers

The OPL contains the synapses of the photoreceptors and here they connect to the dendrites of bipolar- and horizontal cells. There are several types of bipolar cells and they connect the photoreceptor with the ganglion cells. The horizontal cells are interneurons and are called so because their nerve fibres spread horizontally. They connect the photoreceptors to each other and interact with bipolar cells. There are two types of photoreceptors in the human retina, rods and cones, whose nuclei and axons (Henle fibres) form the ONL. The rods and cones consist of an inner and outer segment (IS/OS). The IS of the photoreceptor is divided from the cell nucleus by the ELM. There are about 4.6 million cones in the retina and the density is highest in the fovea and then gradually decreases (Curcio, Sloan, Kalina, & Hendrickson, 1990). The central foveal cone density varies between 100 000 and 324 000 cones/mm^2 among individuals. In the foveola, which is the central part of the fovea, there are only cones

present. These cones are elongated to increase the density and this rod-free area is about 0.350 mm in size horizontally (Curcio et al., 1990). The rods are more numerous than the cones and an average human retina contains 92 million rods. The rods have their highest density around the optic disc and then decrease slowly to the peripheral retina (Curcio et al., 1990). The rods are activated in dim luminance (scotopic vision) conditions while the cones are involved in distinguishing small details in high luminance (photopic vision) conditions and colour vision. Since there are only cones present at the centre of the fovea and the density of cones is highest, this is where the highest resolution is obtained. There are three types of cones and they are sensitive to short (blue), medium (green) and long (red) wavelengths (Kolb, 2007).

The RPE is a single layer of heavily pigmented cuboidal epithelial cells closest to the choroid. The RPE has many functions such as supporting the photoreceptor with nutrition and to remove waste products (Schraermeyer & Heiman, 1999).

2.4 RETINAL DEVELOPMENT

In early foetal life, around FW 6-7, the retina differentiates into two layers, the inner and outer neuroblastic layer. The inner neuroblastic layer forms the ganglion cells, amacrine cells and Müller cells and the outer neuroblastic layer forms the horizontal cells, bipolar cells and photoreceptors (cones and rods) (Mann, 1964; O'Rahilly, 1975). The ganglion cells, horizontal cells and cones are the first retinal cells to be created around FW 8. They are first seen in the fovea and later in the periphery after mid-gestation. Amacrine cells appear a bit later, around FW 10, and finally the bipolar cells, rods and Müller glial cells. After mid-gestation there are no new cones generated while the rod generation continues in the peripheral retina up to 3 months after birth (Hendrickson, 1994). The inner plexiform layer (IPL) first appears in FW 8 and reaches the nasal and temporal peripheral edges by midgestation. The outer plexiform layer (OPL) appears at FW 11 and reaches the edge of the retina by FW 30, thus slower than the IPL (Hendrickson, 2016). By 7 months the retina (except the macula) has almost the arrangement and proportions as an adult (Mann, 1964). The macula continues to develop even after birth.

2.5 FOVEAL DEVELOPMENT

The central part of the retina is the macula and the central part of the macula is the fovea. Histological studies show a rapid development of the human fovea during early life with a maturation process starting at FW 22 and continuing several years after birth (Hendrickson & Yuodelis, 1984; Yuodelis & Hendrickson, 1986; Hendrickson, Possin, Vajzovic, & Toth, 2012). The development of the fovea consists of different stages: extrusion of the inner retinal layers towards the periphery, migration of photoreceptors to the centre of the fovea, elongation of the foveolar cones and reduction of the foveolar cone width to increase packing density (Yuodelis & Hendrickson, 1986; Hendrickson et al., 2012). Between FW 25 and 37

the foveal pit formation is intense and is the result of the displacement of the IRL from the foveal center (FC) towards the periphery. The foveal pit becomes wider and deeper after birth (Hendrickson et al., 2012). Before 28 weeks of GA the total retinal thickness at the FC decreases at a rate of ~14 µm/week and later by ~3 µm/week (Wang, Spencer, Leffler, & Birch, 2012). The maturation of the inner retina is thereby characterized by increased foveal depth and extrusion of the inner retinal layers, resulting in increased thickness of the foveal wall. The maturation of the outer retina is characterized by central migration of photoreceptors to increase foveal cone density and thus creating a thicker ONL. The outer segment of the foveal cones decrease in diameter and increase in length after birth (Hendrickson et al., 2012; Vajzovic et al., 2012).

Studies have shown that the virtual biopsy displayed by the OCT has been proven to correlate well with retinal anatomy known from histological findings (Dubis et al., 2012; Vajzovic et al., 2012). By merging data based on OCT imaging and histological samples, Sjöstrand and Popovic (2013) were able to demonstrate different maturation time frames for the inner and outer retina. The inner retina matures during the late part of gestation, around full term birth, and the outer retina during the first postnatal years. According to Lee et al. (2015), the IRL and ORL continue to develop after birth. The regression of the IRL from the fovea continues until ~17.5 months and the increasing thickness of the ORL reaches maturity at ~75 months. In the IRL, the GCL regresses first from the fovea, followed by the INL, OPL (included in the IRL in this study) and IPL and in the ORL, the IS matures first followed by the OS, ONL and RPE (Lee et al., 2015). The fovea is fully developed around the age of 13-16 years (Hendrickson et al., 2012; Vajzovic et al., 2012).

2.6 RETINAL VASCULARISATION

The development of the retinal vascular structure is complex. Temporary physiological hypoxia (Chan-Ling, Gock, & Stone, 1995) and vascular endothelial growth factor (VEGF) expression are components identified as being associated with the spread of the retinal vasculature (Provis et al., 1997).

Retinal vascularisation begins around FW 15 (Ashton, 1970; Provis et al., 1997; Hughes, Yang, & Chan-Ling, 2000) and the vascular development continues in a complex interaction with the retinal neural development and is finished around full term birth (Hughes et al., 2000). The retinal blood vessels expand from the optic disc to the periphery (Provis et al., 1997). The fovea remains avascularised, creating the foveal avascular zone (FAZ) at around FW 25 (Hughes et al., 2000; Provis & Hendrickson, 2008). The FAZ diameter has been found to correlate with GA and birth weight (BW) (Mintz-Hittner, Knight-Nanan, Satriano, & Kretzer, 1999; Falavarjani et al., 2017). Provis, Billson and Russell (1983) showed that the retinal vascularization seems to coincide with the maturation of retinal ganglion cells, probably due to the increasing oxygen demands of the developing retinal cells (Chan-Ling et al., 1995).

2.7 RETINAL IMAGING

2.7.1 Heidelberg retina tomograph

The Heidelberg retina tomograph (HRT) is a confocal laser ophthalmoscope, which was initially designed for measurement of the optic nerve head structure. It provides images of the optic disc in 3D. The HRT1 was developed in 1991 and was used for research. The HRT2 was developed in 1999 to be used in a clinical setting and the HRT3 was developed in 2005 (including more advanced software), especially for detection and progression of glaucoma (Maslin, Mansouri, & Dorairaj, 2015). The HRT3 contains a retina module for evaluation of the retinal thickness at the macula. It creates a complete topography over the scanned area and gives thickness values in a nine-zone grid (see Figure 3) and in addition an edema index. A typical edema index value in healthy subjects is around 1, whereas index values above 2 are suspicious for an edema. The HRT3 uses a diode laser (670 nm wavelength) to scan the retina point by point and utilizes light reflected from specific depths to create a 3D image of the retina. It creates several 2D scans that combine to one 3D image. The scanning is repeated 3-8 times to create three 3D images with good quality to be combined into a final 3D image of the retina, which is used for analysis (Retina Module, Premium Edition, Heidelberg retina Tomograph3, Operating Manual 19944-E01, Software Version 2.0. December 2006, Heidelberg Engineering GmbH).

2.7.2 Optical Coherence Tomography

2.7.2.1 Technique and development

In 1991, Huang and co-workers described a technique called optical coherence tomography (OCT). The OCT makes cross-sectional images by measuring the optical reflection of structures in biological tissue. The authors concluded that OCT is a promising technique for both basic research and clinical applications (Huang et al., 1991). Two years later Swanson et al. (1993) imaged the optic nerve head and macular region of the retina in vivo with OCT. Since the technique was first the described, it has developed intensely and it is today frequently used to evaluate and manage retinal diseases such as macular holes, epiretinal membranes, macular oedema, vitreomacular traction and glaucoma.

The principle of the technique is similar to ultrasound but uses light instead of sound. A low-coherent near-infrared light (typically 830nm) generated by a super luminescent diode is split into two beams by a beamsplitter. The sample beam is backscattered by the retina and the reference beam is reflected by a reference mirror (Huang et al., 1991). The early type of the technique, called time domain (TD) OCT, used a moving reference mirror to change the path length of the reference beam. When the sample beam and reference beam interference patterns match a signal is detected by the photodetector and processed into an A-scan. Several

longitudinal A-scans at lateral locations provide a cross-sectional two-dimensional image called a B-scan, a form of in vivo histology (Jaffe & Caprioli, 2004).

The moving reference mirror was a relatively slow and mechanical process that limited the amount of data that could be captured (400 A-scans/second) and the image quality and resolution was limited to about 10 µm. The next generation of OCT, called spectral domain (SD) OCT, used a fixed mirror and the photodetector was replaced by a spectrometer (Gabriele et al., 2011). The SD-OCT increased the number of A-scans per second to 80 000, increased the speed of the examination and enabled high resolution images. The SD-OCT was also able to obtain 3D images (C-scans). The newest OCT devise is called swept-source OCT and uses a swept laser with a tunable wavelength and a photodetector. It has improved image penetration by using a wavelength of 1050 nm, axial resolution is around 5µm and the number of A-scans/second is over 100 000 (Fujimoto & Swanson, 2016). The swept-source OCT is a useful device for performing OCT angiography that can visualise retinal vasculature by analysing light reflectance of moving red blood cells (Lavinsky & Lavinsky, 2016).

2.7.2.2 Parameters to measure and repeatability

The OCT is used to examine and evaluate the retinal thickness in the macula and the retinal nerve fiber layer (RNFL) thickness around the optic disc. The average thickness of the macula is given in nine sectors (see Figure 3), i.e. the standardized ETDRS grid, defined by the Early Treatment Diabetic Retinopathy Study (ETDRS). The software also provides tissue volume and cross sectional images (B-scans). Studies have reported good repeatability and reproducibility for both measurements of the optic disc and macular thickness (Pierro, Giatsidis, Mantovani, & Gagliardi, 2010; Brautaset, Birkeldh, Rosén, Ramsay, & Nilsson, 2014). Central macular thickness was ~205µm with the Stratus OCT, 254 µm with the Cirrus OCT (Pierro et al., 2010) and 268µm with Cirrus OCT (Brautaset et al., 2014). Both these studies conclude that different OCT instruments should not be used interchangeably. Stratus TD-OCT measures the retinal thickness between the vitreoretinal border and the IS/OS junction of the photoreceptors but the Cirrus SD-OCT measure the retinal thickness between the ILM and RPE.

Figure 3. The thickness regions according to the 9 areas originating from the Early Treatment Diabetic Retinopathy Study Group.

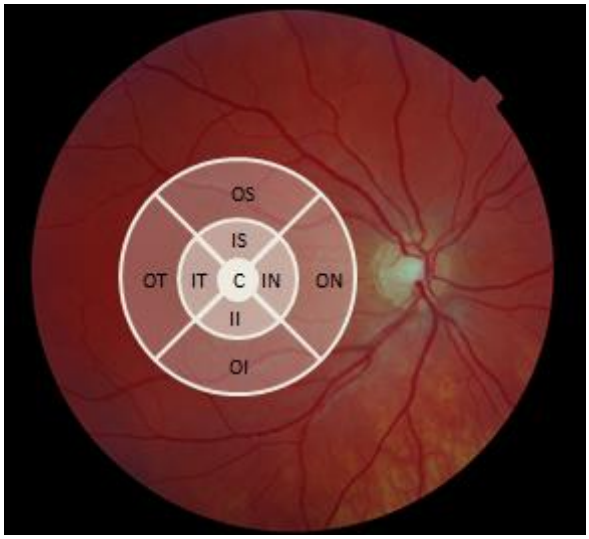

C: centre, IS: inner superior, IN: inner nasal, II: inner inferior, IT: inner temporal, OS: outer superior, ON: outer nasal, OI: outer inferior and OT: outer temporal. The 9 areas can be divided into a central circle (C), an inner circle (IS, IN, II and IT) and an outer circle (OS, ON, OI and OT). Figure from the published article by Brautaset et al., (2015). *Biomed Res Int*, 2015;2015:832863.

2.7.2.3 Possibilities and limitations

Some SD-OCT use noise reduction technology to improve the resolution and an eye-tracking mode to minimize artefacts caused by eye movement (Lavinsky & Lavinsky, 2016). This entails less noise and increases detection of subtle defects in the retina. The fixation control is useful, especially in patients with limited ability to cooperative or to fixate properly.

More advanced techniques have also made it possible to segment different layers in the retina and measure the thickness of those layers, e.g. the individual RNFL and combined GCL+ IPL (GCL+). The OCT image can be displayed in both grayscale and in color.

There are some limitations with the OCT e.g. axial resolution is dependent on the bandwidth and wavelength of the incident light (Jaffe & Caprioli, 2004). The first generation OCT had a lower resolution that did not reveal small structures or defects in the retina. Opacities in the ocular media, blinking, eye movements and low signal strength can also effect the measurement and image quality. These conditions often results in falsely reduced thickness values which makes the mean- and volumetric values less reliable (Hardin, Taibbi, Nelson, Chao, & Vizzeri, 2015). Lateral measurements might differ between subjects with different axial length. As the apparent size of the retinal area measured is magnified in hyperopic eyes (short axial length) and minified in myopic eyes (long axial length), Hirasawa, Shoji, Yoshii and Haraguchi (2014) have suggested adjusting measurements depending on the axial length.

2.8 RETINAL LAYERS IMAGED BY OCT

Different retinal layers have different reflectivity which makes it possible to detect and differentiate them with OCT, see Figure 4. This section will give an overview of the retinal layers imaged by OCT in relation to conventional histology.

Figure 4. A nasal retinal OCT image (B-scan) with the layers labelled on the right. This image is created by adding several straight and tilted B-scans (captured in high-definition) to improve the resolution, image quality and visualizing Henle fibre layer (HFL).

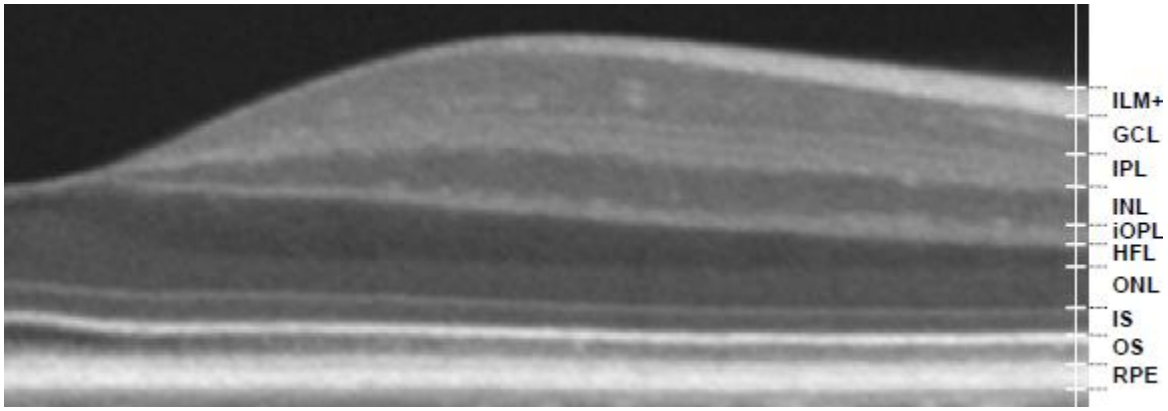

The layers are from top to bottom: (ILM+)-inner limiting membrane and nerve fibre layer (NFL), ganglion cell layer (GCL), inner plexiform layer (IPL), inner nuclear layer (INL), internal part (i) of outer plexiform layer (OPL), Henle fibre layer (HFL), outer nuclear layer (ONL), inner segment layer (IS), outer segment layer (OS) and retinal pigment epithelium layer (RPE). Courtesy of Z. Popovic.

The ILM is hyperreflective and appears white in a grayscale OCT image. When tightly attached to the NFL, which is also highly reflective, they are difficult to separate. In Figure 4 these layers are referred to as ILM+. The inner border of the GCL is easy to detect due to lower reflectivity compared to the NFL. However, the outer border is difficult to separate from the IPL since they have similar reflectivity on standard OCT images. The INL is visible since it is hyporeflective and is surrounded by the hyperreflective layers OPL and IPL. The OPL is hyperreflective on an OCT image and contains photoreceptor synapses. The axons of the photoreceptors (Henle fibres) are obliquely orientated, an organisation that gives the structure low reflectance on standard OCT images. Due to the difficulty in visualising the Henle fibres, it is often included as part of the ONL in OCT anatomical nomenclature. However, when the entry position of the measurement beam is displaced from the pupil center, the reflectance of the HFL changes and becomes either hyper-reflective or hypo-reflective depending on the entry position. When the HFL is hypo-reflective, the true ONL is also visible (Otani, Yamaguchi, & Kishi, 2011; Lujan, Roorda, Knighton, & Carroll, 2011), see figure 4, and this is important in comparison between an OCT scan and histologic section. The nuclei of the rods and cones are placed in the hyporeflective ONL. The rods and cones consist of an inner and outer segment (IS/OS). The ELM divides the IS of the photoreceptor

from the nuclei of the rods and cones which are placed in the hyporeflective ONL. In an OCT image, the ELM and the IS/OS junction are clearly visible since both these bands are highly reflective (Spaide & Curcio, 2011). In the foveola, the central part of the fovea, the cones are elongated and the IS/OS peak formation is an important anatomical landmark in identifying the foveola in an OCT scan. The contours of the foveal depression and the foveal walls are easily recognized with OCT. A normal ratio between the foveal depth and the foveal wall maximum in a normal eye is 1:3 (Tick et al., 2011; Rosén, Sjöstrand, Nilsson, & Hellgren, 2015). The RPE is a hyper reflective single layer of pigmented epithelial cells and appears as white distinguished band on an OCT image (Spaide & Curcio, 2011).

2.9 PREMATURITY AND VISION

Birth before gestational week 37 is defined as prematurity and birth before gestational week 28 is defined as extreme prematurity according to the World Health Organization. There are around 115 000 to 120 000 infants born in Sweden each year and in 2016 around 0.3 % were born before GA of 28 weeks according to the Swedish medical birth register (Socialstyrelsen, 2018). Due to better neonatal care, there is a steadily increasing survival rate of extremely premature infants (Fellman et al., 2009). Studies have shown that preterm children are at higher risk of having reduced visual acuity and refractive errors compared to full term children (Holmström, Azazi, & Kugelberg, 1999; Larsson, Rydberg, & Holmström, 2003; Haugen, Nepstad, Standal, Elgen, & Markestad, 2012; Hellgren et al., 2016). Children born prematurely are at risk of suffering injury to the immature brain (GA 24-34 weeks). The lesions typically occur in the periventricular region. These lesions and their end stage are referred to as white matter damage of immaturity (WMDI). The most common forms of WMDI are periventricular leukomalacia and intraventricular haemorrhage (IVH). Children born prematurely sometimes have multiple lesions (Jacobson & Dutton, 2000). The end-stage lesion, WMDI, may affect motor pathways and cause spastic cerebral palsy, often bilateral. The lesion often affects the optic radiation unilaterally or bilaterally, causing cerebral visual dysfunction (Jacobson & Dutton, 2000). Visual dysfunction due to WMDI may be mild with only slightly subnormal visual acuity or, in the other end of a spectrum, severe with very low or not-measurable grating acuity. Crowding is common and there is a risk of overestimating visual function when only single optotypes are used for acuity testing (Jacobson & Dutton, 2000). The visual field might be reduced in both hemifields and the inferior fields are typically affected (Jacobson, Flodmark, & Martin, 2006; Hellgren, Hellström, & Martin, 2009). Eye motility findings in children with WMDI are strabismus and nystagmus. Ocular findings are either small optic discs or normal-sized optic discs with large cupping caused by retrograde trans-synaptic degeneration of retinal ganglion cells (Jacobson, Hellström, & Flodmark, 1997; Lennartsson, Nilsson, Flodmark, & Jacobson, 2014; Lennartsson, Nilsson, Flodmark, Jacobson, & Larsson, 2018). Children born with low BW are at higher risk of having cerebral visual impairment (CVI) which is one of the most common causes of severe visual impairment in children (Rahi & Cable, 2003). Children with CVI caused by WMDI often have cognitive and perceptual impairment that might cause difficulties in judging depth,

movement perception, recognizing familiar faces, identifying someone they know in a crowd and problems finding their way around which may cause problems in their daily life (Jacobson & Dutton, 2000).

2.10 RETINOPATHY OF PREMATURITY

Since the vascular development of the retina proceeds until ~40 weeks GA, prematurity might cause an interruption of the process and cause the vision threatening disease retinopathy of prematurity (ROP).

The disease ROP has two phases. The exposure to higher levels of oxygen (hyperoxia) outside the uterus leads to a suppression of growth factors and this inhibits retinal vascularisation (phase 1). This leaves the peripheral retina avascularised. When the retina matures the metabolic demand increases, which results in peripheral hypoxia. This leads to expression of growth factors that stimulate retinal neovascularisation (phase 2), which can cause retinal detachment (Chen & Smith, 2007; Hellström, Smith, & Dammann, 2013).

Retinopathy of prematurity is diagnosed through ophthalmoscopy and the disease is divided into five stages based on the ophthalmoscopy findings. The stages mirror the severity, i.e. the progress of the abnormal retinal vascular development.

Stage 1 is defined by a demarcation line between the avascular retina and the vascularised retina. In stage 2 the demarcation line in stage 1 has grown in height and width into a ridge that extends from the plane of the retina. Stage 3 is defined by the presence of fibrovascular proliferation, stage 4 is partial detachment of the retina and stage 5 is defined by total retinal detachment (The Committee for the Classification of Retinopathy of Prematurity, 1984; International Committee for the Classification of Retinopathy of Prematurity, 2005). The first two stages often regress spontaneously. Stage 3 can regress spontaneously but might require treatment in case of progression.

Treatment of ROP is based on destruction of the peripheral retina in order to decrease the triggering of pathologic vascular growth. In the 1980s, the treatment of ROP consisted of cryotherapy of the peripheral retina. Nowadays, laser photocoagulation treatment has replaced cryotherapy and treatment is performed according to the Early Treatment for ROP study (Early Treatment For Retinopathy of Prematurity Cooperative Group, 2003). Treatment with anti-VEGF injections has been used during recent years, but this is still controversial since long-term effects are not known and further studies are needed (Sankar, Sankar, & Chandra, 2018).

In Sweden, all children born at gestational age of 30 weeks + 6 days or less are screened for ROP. Between 2008 and 2012 the prevalence of ROP in preterm infants was 30.3% and 5.2% required treatment. The incidences of ROP and frequencies of treatment were similar during the study period (Holmström et al., 2016).

Preterm children treated for ROP have steeper corneal curvatures, shallower anterior chamber depths, thicker lenses and higher degrees of refractive errors but no difference in axial length compared to preterm children with mild/no ROP and full-term children (Wu et al 2012; Lee et al., 2018).

2.11 EXTREMELY PRETERM INFANTS IN SWEDEN STUDY (EXPRESS)

The EXPRESS study (Extremely Preterm Infants in Sweden Study) is a national collaboration project, a prospective and population-based study, with the aim to investigate the short and long-term morbidity of children born at GA <27 weeks. Data from all infants born extremely preterm were collected by the 7 health care regions in Sweden.

From April 1, 2004 to March 31, 2007 there were 305 318 infants born in Sweden, 1011 of these were born extremely preterm, 707 were live-born and 70% survived to 1 year. With increased GA the number of infants born and live-born increased. The perinatal mortality ranged from 93% in infants born at GA 22 weeks to 24% in infants born at GA 26 weeks (Fellman et al., 2009).

During the neonatal period the children born EPT underwent screening for ROP and graded according to the Classification of retinopathy of prematurity and treatment was performed according to the recommendations of the Early Treatment for retinopathy of prematurity study. Intraventricular haemorrhage (IVH) was classified as no, mild (stage 1 and 2) and severe (stage 3 and 4) IVH according to Papile, Burstein, Burstein & Koffler (1978) (Fellman et al., 2009).

In 2009, a study was published about the incidence of ROP in the children born EPT and the results showed that 73% had ROP, mild ROP was present in 38%, severe ROP was present in 35% and treatment was performed in 20%. Both GA and BW were related to severe ROP, but GA was more associated than BW (Austeng, Källen, Ewald, Jakobsson, & Holmström, 2009). Ten percent developed severe IVH (The EXPRESS Group, 2010).

When the children were 6.5 year old they were examined again and 38% of the children born EPT had some ophthalmologic abnormality compared with 6% of the matched control group. Strabismus was found in 17% and refractive errors in 30%, of the preterm children as compared to 0% and 6% in the control children (Hellgren et al., 2016). Cognitive disability was more frequently seen among children born EPT compared to controls (Serenius et al., 2016).

2.12 FOVEAL DEVELOPMENT AFTER PRETERM BIRTH

Foveal structure in children born preterm has been described by several authors. Common findings indicating inhibited foveal development include reduced foveal depth (shallow pit) and incomplete extrusion of inner retinal layers in the FC (Maldonado et al., 2011; Wang et al., 2012; Wu et al., 2012; Yanni et al., 2012), see Figure 5 A-C. However, even in a normal adult population, incomplete extrusion of the IRL at FC has been noted in about 7% of the cases (Tick et al., 2011) and another study showed that cone specialization can be obtained despite the lack of a foveal pit (Marmor, Choi, Zawadzki, & Werner, 2008).

Dubis et al. (2012) studied foveal maturation in preterm infants born at GA ≥32 weeks by the use of OCT. At GA 32, the foveal pit was present and appeared deeper and more distinct with increasing age. Vajzovic et al. (2012) showed high correlation between histologic findings and findings visualised by OCT at all stages of development. At birth, the preterm infants had a shallow pit with IRL at FC and short, undeveloped foveal photoreceptors with no or little signs of outer segment lengthening, i.e. the photoreceptors have not fully migrated to the centre of fovea and increased in length at birth (Maldonado et al., 2011; Vajzovic et al., 2012). A review of data (Sjöstrand & Popovic, 2013) indicates that signs of immaturity in the inner retinal layers are permanent while the outer retina continues to develop after birth and therefore turns out less affected in children born prematurely.

Figure 5A-C. OCT images of a fully matured retina (Fullterm A) and under developed retinas in prematurely born cases B and C. These images are created by adding several straight B-scans (captured in high-definition) to improve the resolution and image quality.

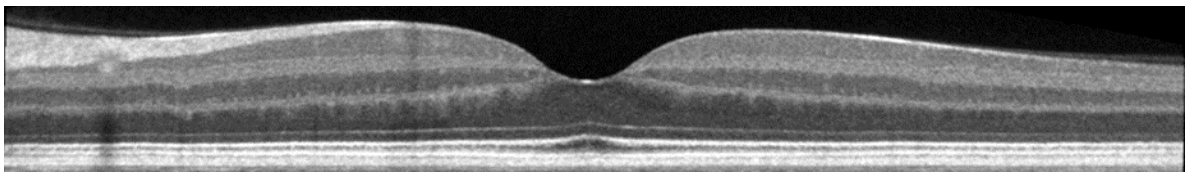

A. Fullterm

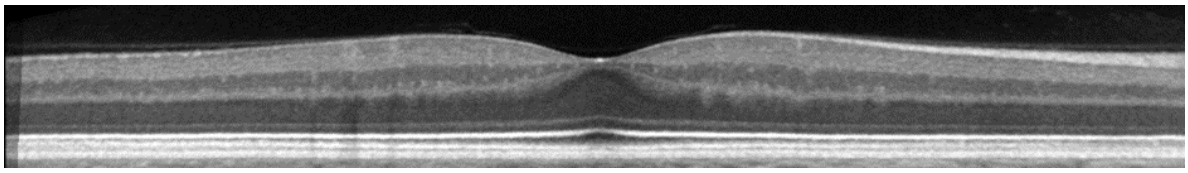

B. Preterm born at GA 30, without ROP

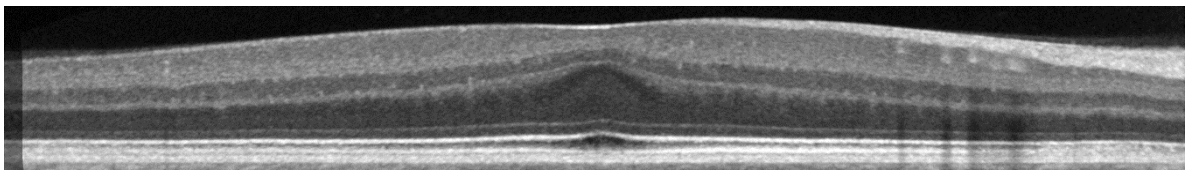

C. Preterm born at GA 24, with ROP that required cryotheraphy treatment

(A) The foveal depth (FD) is more than 1/3 of the thickness compared to the retinal thickness at the foveal wall. There are no IRL in the FC and the IRL free zone is wide. The outer nuclear layer (ONL) bulge is smooth in shape. (B) The FD is reduced, there is no IRL free zone and the ONL bulge is more triangle shaped compared to the fullterm. (C) The foveal pit is nearly absent and all retinal layers are seen at FC, which contributes to an increased central retinal thickness compared to A and B. The ONL bulge is more triangular compared to fullterm. OS lengthening is seen in all images. Courtesy of Popovic, Z.

3 AIMS

- Aims of study I were to evaluate the test-retest variation of macular thickness measurements using the HRT3 Retina Module and compare it with Stratus OCT and to establish reference values for the HRT3 Retina module.
- Aim of study II was to characterize typical microanatomical alterations of immaturity in the fovea, by the use of single SD-OCT B-scan and customized Matlab programe, after extremely preterm birth.
- Aims of study III were to evaluate the retinal thickness, by the use of SD-OCT and statdardized measuring protocol, in a population-based cohort of 6.5-year-old children born EPT in comparison to children born at term and to investigate risk factors associated with the macular thickness in children born preterm.
- Aim of study IV was to evaluate the combined ganglion cell layer and inner plexiform layer in a population-based cohort of children born EPT compared to children born at term by the use of single SD-OCT B-scan and customized Matlab programe.

4 MATERIAL AND METHODS

4.1 STUDY I

Thirty healthy subjects and 30 patients with macular oedema were recruited for the study. To evaluate the test-retest variability, the subjects were examined five times at two different occasions by two experienced examiners. Three measurements were obtained at the first visit (two by examiner 1 and one by examiner 2) and two at the second visit (one by examiner 1 and one by examiner 2). The measurements were compared in four different ways, see Table 1. The patients were examined twice by examiner 1 (intraobserver/intravisit) since they were expected to have changes in macular thickness over time.

Table 1. Analysis schedule.

I	Intraobserver/intravisit	1st examiner then 1st examiner, same visit
II	Interobserver/intravisit	1st examiner then 2nd examiner, same visit
III	Intraobserver/intervisit	1st examiner then 1st examiner, different visits
IV	Interobserver/intervisit	1st examiner then 2nd examiner, different visits

Table approved for reuse by Wiley from the published article by Rosén et al., (2012) *Clin Exp Opto, 95(5),* 515-521.

Inclusion criteria for the healthy subjects were refractive error up to 12.00 Dioptres (D), a visual acuity (VA) $\geq$ 1.0, no systemic disease that would influence the retinal thickness, no ophthalmic disease and an intraocular pressure (IOP) below 21 mmHg. For the patients the inclusion criteria were macular oedema caused by uveitis and refractive error up to 12.00 D. The subjects and patients underwent ophthalmic examination including, auto-kerato-refractometry, VA testing with ETDRS charts and slit-lamp examination. Icare tonometry was used to measure the IOP in all patients and in healthy subjects 40 years and older.

Successful images were obtained in all healthy subjects and in 9 patients with both HRT3 and Stratus OCT. All examinations using the Stratus OCT, of both patients and controls, resulted in good image quality. With the HRT3 only images from 9 patients out of 30 were possible to analyse. The measured retinal area is divided into a 9-zone grid or a macular map that is centred at the fovea in both the HRT3 and Stratus OCT and the retinal thickness is automatically calculated by the software for each of the 9 zones. The macular map consists of a central circle and two concentric circles each subdivided into four quadrants, see Figure 3. Since the standard diameters of the macular map differs between the HRT3 and Stratus OCT the diameters were set to 1 mm, 2.22 mm and 3.45 mm to ensure equal comparisons.

4.2 STUDY II

In study II, a subgroup of 6.5 year-old children who participated in the EXPRESS study were included. The children were consecutively recruited according to GA at birth and organized in 4 groups with 10 children in each: Group A included children born at term, Group B included children born at GA 25-26, Group B* included children 25-26 with ROP stage 3 and Group C included children born at GA 23-24 with ROP stage 3. Two children in Group B* and 8 children in Group C had received treatment for ROP. Macular images were obtained with Cirrus SD OCT from both eyes in all children. The OCT image with highest signal strength and best image quality was selected and a single B-scan including the FC was analysed. Anatomical landmarks were used to ensure that the B-scan represented the FC. The landmarks were: a visible foveal reflex and/or where the maximum foveal depression was found as well as the highest IS/OS peak. The parameters based on normal foveal development events such as formation of the foveal pit, extrusion of the IRL, ONL thickening and OS lengthening were analysed. At the FC the FD, IRL thickness, ONL+ thickness (includes OPL, ONL, ELM and the myoid zone of the photoreceptor inner segment) and OS+ thickness (includes the ellipsoid zone of the photoreceptor inner segment, OS and RPE) were measured. The ONL+ was also measured at the foveal wall maximum (FWM) both nasally and temporally and an average was calculated. All measurements were performed twice manually in Image J to make sure that it was correct and also confirmed by using a custom made Matlab program.

4.3 STUDY III AND IV

The study participants were children born before a GA of 27 weeks and children born at term. The children were 6.5 years old, born between 2004 and 2007 and participated in the EXPRESS study (Fellman et al., 2009). The participating children in study III were born in two health regions (Stockholm and Uppsala) in Sweden and in study IV only children from Stockholm were included. During the neonatal period the children born EPT had undergone screening for ROP. Stage 1 to 2 was defined as mild ROP and stage 3 to 5 as severe ROP. In study IV the children born EPT with severe ROP were divided in two groups: severe-untreated (ROP Stage 3) and severe-treated (ROP Stage 3-5). Intraventricular haemorrhage (IVH) was classified as no, mild and severe IVH.

Macular Cirrus SD-OCT examinations were performed in all children. Monocular visual acuity was tested with habitual correction using LogMAR Lea Hyvärinen symbols. Spherical equivalent (SE) was calculated from refraction measured with automated refractor with cycloplegia. The examinations were performed between 2010 and 2014. In study III the macular retinal thickness in the nine ETDRS areas was measured and analysed together with risk factors associated with a preterm birth and sex. The ETDRS areas were divided into a central circle, an inner circle and an outer circle, see Figure 3. In study IV one B-scan at the FC were selected for further analyses. Retinal segmentation was done with custom software

written in Matlab. The inner border of GCL, outer border of IPL (GCL+) and FC were marked manually. To make sure that the segmentation was correct it was made twice in all images and the consistency was found to be high. Based on the maximum GCL+ thickness at the nasal (N) and temporal (T) side and the position of the FC, 11 landmarks were obtained automatically, as shown in Figure 6.

Figure 6. OCT image with landmarks and plotted GCL and IPL boundaries from a child born at term.

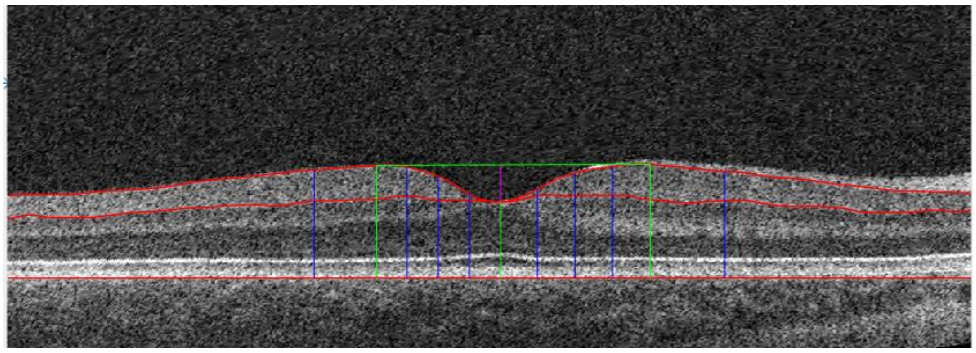

Purple line is FD, central green line represents the FC, peripheral green lines represent regions with maximum nasal and temporal GCL+ thickness, and blue lines represent the 1.5, 0.75, 0.5 and 0.25 landmarks both temporally and nasally between FC and rim. Red lines represent the borders of inner GCL, outer inner plexiform layer and outer retinal pigmented epithelium. Figure from study IV.

The average GCL+ thickness was evaluated in 4 regions, 1.5N to 1.5T (total), 0.5T to 1.5T (temporal), 0.5N to 1.5N (nasal) and 0.25N to 0.25T (central). The N rim to T rim (rim distance) and FD was also obtained. These parameters were analysed together with risk factors associated with a preterm birth and sex.

4.4 STATISTICAL METHODS

A p-value <0.05 was considered significant for all analyses.

In study I, Microsoft Office Excel 2007 (Microsoft, Redmond, WA, USA) and the IBM SPSS Statistics, version 19 (IBM Corporation, Armonk, NY, USA), were used for analysis and calculations. Repeated ANOVA was used to compare all measurements with HRT and OCT within instruments and between instruments. Pearson correlation was used to analyse correlation between the HRT and OCT data. Repeatability and reproducibility were analysed as a coefficient of variation (CV) and as an intraclass correlation (ICC). Bland-Altman plots were used to show the agreement between measurements with both the HRT and OCT.

In study II, the statistical analyses were performed with InStat version 3.00 and SPSS version 21 (IBM Corp, Armonk, NY). Depending on the distribution of the data in all group comparisons independent Student T-test and the Mann–Whitney U-test were used. Pearson

correlation analysis was performed within the preterm groups. Mean values and standard deviations (SD) were calculated for the different parameters in each group. Pearson correlation was used to analyse the correlation between GA and FD/IRL thickness.

In study III, the statistical analyses were performed with SPSS, version 22 (IBM Corp, Armonk, NY) and R program, version 3.1.1. The mean values and SD were calculated for the macular thickness in each of the 9 ETDRS areas and for the inner and outer circle. When comparing means of continuous data, independent sample T-test was performed. A series of linear mixed models were used for the analysis of the macular thickness. The comparison between the children born EPT and the children born at term was done for each of the three circles (central, inner and outer) using group and eye as fixed factors and subjects as random factor. To evaluate factors related to the macular thickness in the central circle and the inner and outer circles of the preterm children, analyses were performed in two steps. In the first step, simple linear mixed models were performed for a few predetermined independent factors (GA, BW, gender, VA, SE, and presence of previous ROP (present or not) and no, mild or severe IVH. In the second step, factors in the simple linear mixed model with a p-value <0.05 were entered into a multiple linear mixed model.

In study IV the statistical software R, version 3.3.3 was used for all statistical analyses. The function lmer in R-package lmerTest was used to fit linear mixed models. No severe deviations from normality were found when the normality of the outcome variables was visually inspected with QQ-plots. Children born EPT were compared to control children with regards to FD and GCL+ thickness at different retinal positions the outcome variables using linear mixed models with a random intercept for each child, taking into account the within-subject dependency as most of the children born EPT were having outcome measures for both eyes. The models were adjusted for the children's biological sex. For the children born EPT, associations between the outcome variables and sex, gestation days, IVH, ROP and ROP requiring treatment were assessed with linear mixed models, with a random intercept for each child born EPT. Linear correlation between the outcome variables was estimated using linear regression, with cluster robust standard errors taking into account the within-subject dependency and with adjustments made for sex and gestation days.

4.5 ETHICAL CONSIDERATIONS

The regional ethic board approved the studies (DNR 2009/604-31/1 and 2010/850-31/1), which were performed according to the stipulations of the Declaration of Helsinki. Written consent was mandatory for all participants in study I and written parental consent was mandatory for the participation of all children in studies II, III and IV.

The OCT is a non-invasive, non-contact investigation with no need for any diagnostic drugs and with the use of "eye-safe" wavelengths there are no ethical concerns related to the technique or measurement itself. However, the multiple examinations may cause stress or be tiring for the patients since they must concentrate and keep the fixation stable. This could be

demanding for a patient with reduced vision as in study I or especially children as in study II-IV. Children need special consideration and at an age of 6.5 years the personal motivation and understanding of the benefits of taking part of scientific studies might be limited in some cases. On the other hand, many of the prematurely born children are at risk of having visual problems that are of great importance to understand in order to be able to offer support and help, e.g. help during school time. An OCT measurement only takes a few minutes and the subjects were seated comfortably during testing. However, during the examinations we have carefully tried to motivate the children in a way that is understandable to them and respected any will to discontinue with the examination. No children have been encouraged by offering bribes. We had limited the time to 5-10 minutes and tried to make the children interested in the camera (OCT machine) by offering them to examine their parents before being examined themselves. Normally there is no or minimal risk of feeling tired afterwards. Another aspect is that parents might always feel frightened of "something new" being discovered. Therefore all our subjects and their parents have been carefully informed by a highly experienced ophthalmologist during their visits. In the end, it was surprising how positive, curious and cooperative the children turned out to be.

5 RESULTS

5.1 STUDY I

No significant differences in mean macular thickness within any of the areas between different sessions were found within any of the techniques. Mean macular thickness in all areas measured with the HRT3 was significantly thicker compared with the Stratus OCT and no significant correlations were found between the techniques in any area. The coefficient of variation (CV) was calculated for each area and ranged from 4.5% to 8.8% with HRT3 and from 0.6% to 1.5% with Stratus OCT in healthy subjects. The central area had the largest CV (8.8%) measured with HRT3 by different examiners at different visits (IV) and the CV with Stratus OCT showed 1.0% for the same session and area. Outer nasal area measured by the same examiner at the same visit (intraobserver/intravisit) with Stratus OCT had the smallest CV (0.6%) and HRT3 showed 7% for the same session and area. The CV ranged from 7.9 to16.6% with HRT3 and from 1.1 to 2.5% with Stratus OCT in the 9 patients with macular oedema. The ICC in the central area for intraobserver/intravisit (I) was 0.78 with the HRT3 and 0.93 with the Stratus OCT in healthy subjects. Corresponding values were 0.64 with the HRT3 and 0.99 with the Stratus OCT in patients with macular oedema. The ICC was 0.73 with the HRT3 and 0.97 with the Stratus OCT in the healthy subjects for interobserver/intervisit (IV). Bland-Altman plots showed a larger variation between measurements with the HRT3 compared with the Stratus OCT.

5.2 STUDY II

Children born EPT had significantly shallower FD (-53µm), thicker IRL (22µm) and thicker ONL+ (24µm) at the FC compared to children born at term. No difference regarding the OS+ thickness was found, see Figure 7A-D.

Figure 7 A-D. Standard OCT images of a child born at term (A) and children born preterm at different gestational age (GA) (B, C and D).

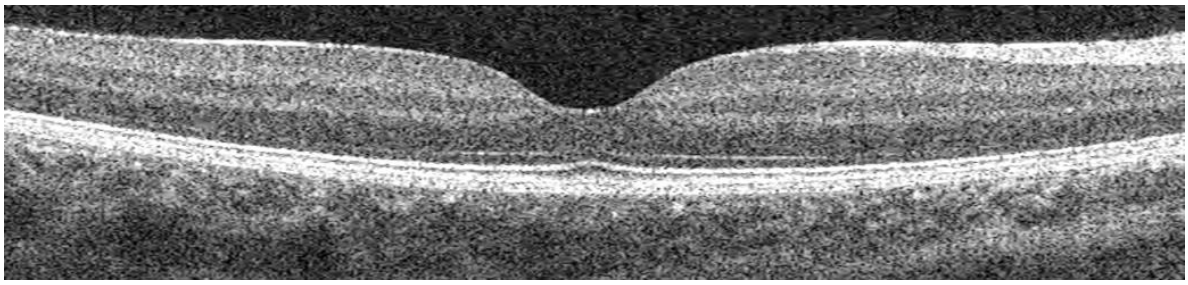

A. Fullterm

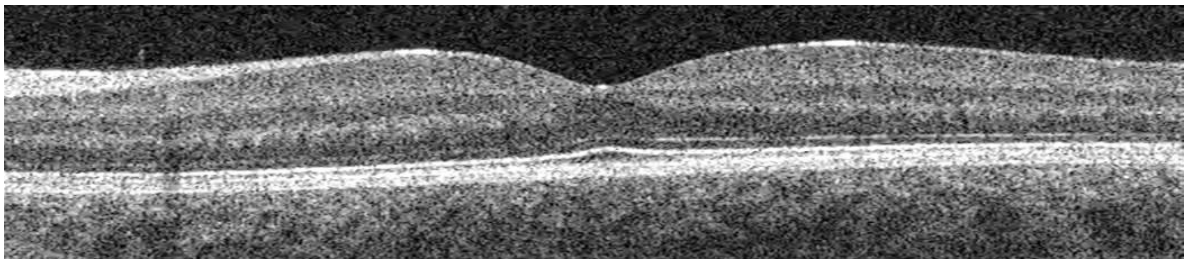

B. Preterm born at GA 26 without ROP

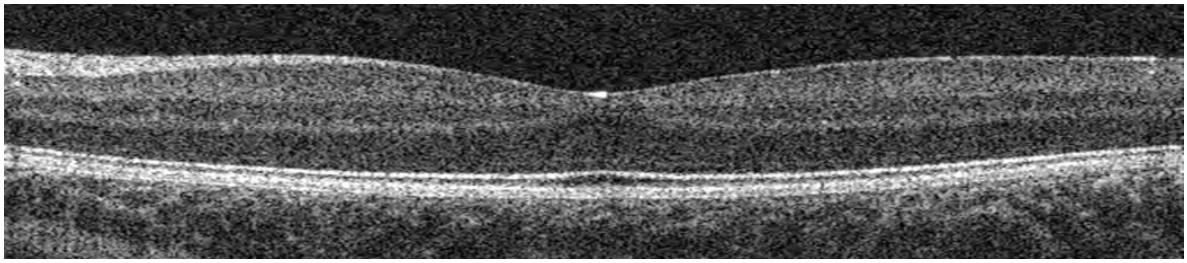

C. Preterm born at GA 25 with ROP 3 that required treatment

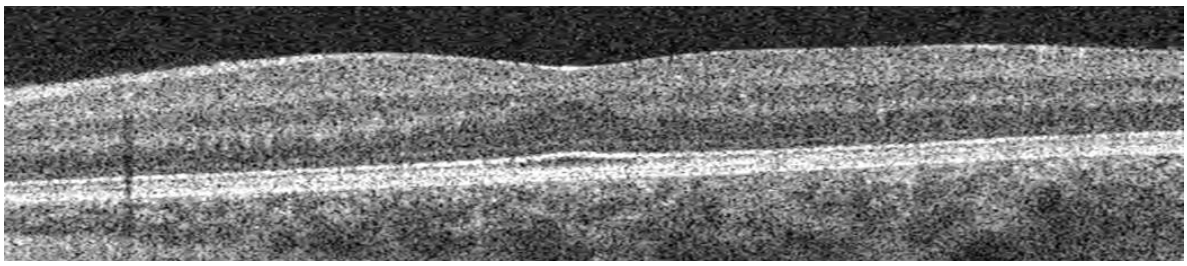

D. Preterm born at GA 23 with ROP 3 that did not require treatment

Notice the shallow FD, IRL thickness at the FC and the shape of the ONL in the children born EPT. ROP=retinopathy of prematurity.

A FD equal or larger than one-third (considered as normal) of the foveal rim thickness was seen in 9 out of 10 children born at term, see table 2. Foveal depth and GA correlated significantly ($r=0.53$; $p = 0.003$), and a negative correlation between IRL thickness in FC and GA ($r=-0.43$; $p = 0.017$) was found. The FD increased steeply with 14µm per week and the IRL thickness decreased with 8 µm per week during GA 23 to 26. The children born at GA 25-26 without ROP (Group B) had a significant shallower FD and ONL thickness compared to children born at term. No differences could be found in any of the measured parameters between children born at GA 25-26 without ROP (Group B) and children born at GA 25-26,

with ROP Stage 3 (Group B*) or between Group B* and children born at GA 23-24, with ROP Stage 3 (Group C).

The control subjects had a well formed foveal pit and the main part of the IRL was extruded in all subjects but one and the shape of the ONL+ were wide and broad. The premature children (GA 23-24) showed an arrested development of the foveal pit and incomplete extrusion of the IRL in all subjects but one and in some subjects the ONL+ shape was steep and triangle shaped. The children born EPT without ROP (Group B) and children with ROP Stage 3 (Group B*) were compared to evaluate the impact of ROP. The foveal pit was present in all subjects but clearly arrested in 3 subjects in each group. Most subjects had incomplete extrusion of the IRL in Group B and in all cases except one in group B*.

Table 2. Foveal depth and IRL thickness at FC in % of the average (nasal and temporal) total retinal thickness at FWM.

Group	FD (%)	IRL (%)	FWM (µm)
A (n=10)			
Mean±SD	37±6	4.3±5.6	347±17
Range	27-46	0-15.6	316-378
B (n=10)			
Mean±SD	28±6	8.0±6.6	339±10
Range	16-36	0-15.2	316-350
B* (n=10)			
Mean±SD	23±5	10.5±6.0	340±14
Range	16-32	0-17.9	324-362
C (n=10)			
Mean±SD	18±9	15.7±7.3	329±14
Range	6-35	0-27	302-341

A=controls, B= GA 25-26, without ROP, B*= GA 25-26, with ROP Stage 3 and C= GA 23-24, with ROP Stage 3. n=number of eyes, SD=standard deviation, FD=foveal depth, IRL=inner retina layers, FWM= foveal wall maximum, ROP=retinopathy of prematurity, GA=gestational age.

5.3 STUDY III

Sixty-seven percent (134/199) of the children born EPT and 90% (145/162) of the children born at term were successfully imaged with the OCT in at least one eye. The GA was significantly lower in the EPT dropout group compared to the participating EPT group (mean difference -0.4 weeks). Children born EPT had significantly thicker central macula with 34µm compared to children born at term, even when adjusted for sex. The central macular thickness was reduced by approximately 4µm/gestational week. A thicker central macula was associated with low GA, history of ROP (7µm) and male sex (9µm). Children with severe IVH had a significant thinner retina (-17µm) in the inner circle compared to children born ETP without or with mild IVH. Children born EPT had significantly lower VA ($p<0.001$) but no difference in SE compared to children born at term. Neonatal data, clinical data and central macular thickness (central circle) are shown in Table 3.

Table 3. Neonatal data, clinical data and central macular thickness.

	EPT	Control
GA Mean (SD) Range	25.0(1.0) 23-26	40.0(1.1) 37-41
Sex girls/boys (%)	57(43)/77(57)	62(43)/83(57)
VA RE Mean (SD) Range VA LE Mean (SD) Range	0.82(0.23) 0.02-1.25 0.86(0.20) 0.03-1.25	0.97(0.16) 0.4-1.25 0.98(0.17) 0.63-1.60
SE RE Mean (SD) Range SE LE Mean (SD) Range	+1.42(1.98) -11.13 to +7.50 +1.34(2.15) -9.38 to +7.38	+1.33(0.90) -1.00 to +6.13
CC RE Mean (SD) CC LE Mean (SD)	282(20) 283(21)	249(19) 248(18)
ROP(%) No/Mild/Severe Treatment	 36(27)/55(41)/43(32) 18(13)	
IVH(%) No/Mild/Severe	 81(60)/43(32)/8(6)	

GA=gestational age in weeks, VA=decimal visual acuity, SE=spherical equivalent in Dioptres, RE=right eye LE=left eye, CC=central macular thickness in µm, ROP=retinopathy of prematurity, IVH=intraventricular haemorrhage.

5.4 STUDY IV

The total GCL+ was 5 µm thicker in the 89 children born EPT compared to the 92 control children. The largest difference was seen in the central part of the macula (central GCL+) where the children born EPT was 21 µm thicker. No differences were seen at the nasal or temporal side. Children born EPT had a reduced FD with -53µm compared to children born at term. The parameters with significant differences were further analysed within the EPT group to study any association with sex and the outcome variables GA, ROP and IVH which are related to preterm birth.

The central GCL+ thickness was reduced with 2.8 µm per week and the FD increased with 9.8 µm per gestational week from GA 23 to 26. The central GCL+ thickness and FD was associated with male sex, GA, ROP and ROP treatment. The total GCL+ thickness was associated with having severe treated ROP and severe IVH, see Table 4.

Correlations

There was a correlation between decreased FD and increased central GCL+ thickness (r=-0.75) within the EPT group and within the control group (r=-0.44). The correlations remained significant after adjusting for sex and GA. Within the EPT group a weak correlation was seen between VA and the outcomes FD (r=0.25, p=0.005) and central GCL+ thickness (r=-0.22, p=0.019). These relations were not found in the control group. The correlations remained significant after adjusting for sex and GA.

Table 4. Variables and outcomes in children born EPT.

Variables	Subgroups	Total GCL+	Central GCL+	Foveal depth
Sex	Boys vs Girls	NS	8.3	-17.6
			3.4 - 13.2	-6.5 - -28.7
Retinopathy of prematurity	Mild vs No	NS	5.9	-12.5
			1.2 - 10.7	-20.4 - -4.6
	Severe_untreat vs No	NS	NS	-12.9
				-23.6 - -2.2
	Severe_treat vs No	4.7	12.7	-27.6
		0.8 - 8.6	5.8 - 19.7	-40.0 - -15.2
	Severe_untreat vs Mild	NS	NS	NS
	Severe_treat vs Mild	4.6	7.0	-15.1
		1.3 - 8.0	0.9 - 12.8	-25.5 - -4.8
	Severe_treat vs Severe_untreat	NS	7.3	-14.7
			0.3 - 14.3	-27.2 - -2.3
Intraventricular haemorrhage	Mild vs No	NS	NS	NS
	Severe vs No	-7.8	NS	NS
		-13.2 - -2.4		
	Severe vs Mild	-7.1	NS	NS
		-12.6 - -1.5		

Estimated mean difference and lower and upper 95% confidence interval in µm. Values are only presented for statistically significant differences, i.e. $p \leq 0.05$. NS = no significant difference, GCL+ = ganglion cell layer + inner plexiform layer. Table from study IV.

6 DISCUSSION

The aim of the first study was to evaluate the test-retest variation for macular thickness measurements with the Retina Module in HRT3 and compare it with the Stratus OCT, a more established method for macular thickness measurements. The results showed no significant difference in macular thickness between the different examinations with any of the methods. However, the two methods gave different thickness values of corresponding retinal areas and did not correlate. The patients with macula oedema had increased macular thickness with both devices. Only 9 patients with macular oedema were imaged with sufficient image quality with the HRT3. Successful measurements were more difficult to get with the HRT3 due to the prolonged examination time and difficulties for the patient to fixate the fixation target. Both examiners found Stratus OCT more user friendly both for the patients and the examiner. With this conclusion and the rapid development of the OCT technique the SD-OCT seemed as a good option to use in future studies when examining children.

The eye examinations of the children aged 6.5 years old in the follow-up EXPRESS study began in 2010 and ended in 2014. A qualitative and quantitative grading system was developed initially, inspired by Thomas et al. (2011), based on normal foveal development. Specific parameters describing this event were used to enable comparisons between groups. Ideally, the aim was to recruit children born EPT at different GA without ROP in order to investigate the isolated impact of GA. However, it was not possible to recruit 10 EPT children born before GA 25 without ROP in the Stockholm regional cohort. In order to make the comparisons between age-groups as sensitive as possible a fourth group (Group B*) was included with children born at GA 25-26 weeks with similar ROP prevalence (Stage 3) to that seen among the subjects in the EPT born at GA 23-24 (Group C). The second study revealed more pronounced deviations in the foveal anatomy in children born before GA of 25 weeks than in those born after. The FD increased gradual with 14µm/gestational week from GA 23 to 26 weeks and the children born EPT had thicker IRL and ONL+ at the FC compared to children born at term. No difference could be found regarding the OS lengthening. Other studies have also shown that the outer retinal layers of the retina generally develops well after preterm birth and signs of immaturity is more pronounced in the IRL (Wang et al., 2012; Yanni et al., 2012). The deviation of the ONL bulge was a novel finding at the time. At first, the increased ONL+ thickness at FC in children born EPT could be taken as sign of maturation. Further investigation of ONL bulge to be steeper and narrower it seemed to be linked to the inhibited migration of the IRL and might be caused by less pulling of their axons by the ganglion cells towards the periphery due to the interrupted extrusion of the IRL at the time of birth (Sjöstrand, Rosén, Nilsson, & Popovic, 2017).

The results from study II showed that a FD less than 1/3 of the average thickness at the FWM (See table 2) and IRL at the FC are signs of an immature fovea. When evaluating the whole EPT group (from the Stockholm cohort) the FD was less than 30% of the average FWM thickness in 78% of children born EPT and all except one had incomplete extrusion of the

IRL at the FC. Among the children born EPT with a pit deeper than 30% of the average FWM thickness, all but one had complete extrusion of the IRL at FC and the majority had no or mild ROP and were born at GA 25-26. Almost all of the control children had a mature fovea but 5 % had signs of an IRL rest at the FC and 2% had a FD less than 30% of the average FWM thickness. All control children and the majority of the children born EPT had visible ELM and IS/OS peak.

The third study gave access to study a large and unique population-based group of EPT children of the same age. This gave an opportunity to study factors associated with prematurity and the connection to foveal maturation. This study showed that children born EPT had a significantly thicker central macula compared to children born at term. Low GA, male sex and ROP were important risk factors for an increased macular thickness. These factors will be discussed further down. The central thickness was motivated to measure since the second study revealed signs of immaturity at the FC and that the FD were most affected of the preterm birth. The third study also revealed that children born EPT with severe IVH had a significantly thinner inner circle compared to children born EPT without IVH or with a history of mild IVH. This might be a result of ganglion cell loss caused by retrograde degeneration of neurons due to IVH-induced damage to the optic radiation (Lennartsson et al., 2014, 2018). Therefore we found it interesting to measure the isolated GCL layer in the macular region. The new version of the software of the OCT was able to measure the GCL+ around the FC at fixed positions but we had no access to this software during the third study. The manual measurements used in the second study were very time consuming but gave valuable information about the maturity of the foveal structure. In the fourth study, the custom made Matlab program for manual measurements was improved to facilitate the evaluation of the retinal structure and GCL+. The Matlab program was able to measure in one single horizontal B-scan and thereby made it possible to include more subjects (compared to study III) since high quality cube measures are difficult to obtain when examining young children. As mentioned the OCT software were also able to measure the GCL+ but frequently fails to segment the true borders of the GCL and IPL at the FC in eyes with incomplete extrusion of the IRL (Nilsson, Hellström, & Jacobson, 2016). The software being based on normal anatomy most likely explains this, and the consequent of the error is falsely reduced values. In addition Sjöstrand et al. (2017) had shown that preterm birth might give a reduced rim distance and these circumstances lead to the use of manual measurement of the GCL+ since it seemed to give more fair comparisons between groups. Our results showed that children born EPT has increased total and central GCL+ thickness and a reduced FD compared to children born at term. Low GA, male sex, and ROP treatment all had some association with increased central GCL+ and reduced FD. As mentioned earlier the third study also revealed that low GA, male sex and ROP were associated with an increased macular thickness. Previous studies have shown an increased central macular thickness, central GCL+ thickness or reduced FD in preterms both with and without ROP compared to term born (Bowl et al., 2016; Nilsson et al., 2016; Wang et al., 2012; Wu et al., 2012; Yanni et al., 2012). The FD increased with 10-14 µm/gestational week and the foveal thickness

decreased with 4 µm. The FD is measured in a single B-scan and the foveal thickness is a mean value of a circle with a diameter of 1 mm so of course they could not be inter-changed. When estimating the FD the thickness at the FWM is taken into account and this might indicate that FD better represent the maturity of the fovea compared to central retinal thickness at the fovea.

The central macular thickness, FD and central GCL+ thickness were influenced by sex, i.e. boys had a thicker central macula, GCL+ and reduced FD compared to girls. Other studies have shown that male sex is associated with increased central macular thickness in healthy adults (Wagner-Schuman et al., 2011), children 4-17 years (Barrio-Barrio et al., 2013) but not to a decreased foveal depth in adults (Wagner-Schuman et al., 2011). Preterm boys are more likely than girls to have neurodevelopment impairment (Hintz et al., 2006.

Previous history of ROP and ROP treatment were also associated with increased macular and GCL+ thickness and reduced FD. Other studies has also revealed that preterms treated for ROP has reduced FD (Wu et al., 2012; Nilsson et al., 2016: Lee et al., 2018), thicker foveal thickness (Wu et al., 2012; Bowl et al., 2016), thicker central GCL+ thickness (Bowl et al., 2016) and thicker macular RNFL+GCL+ thickness (Lee et al., 2018) compared to controls.

The children born EPT had significantly lower VA compared to the children born at term and no association was found between VA and central macular thickness in the third study. This is in line with other studies on preterm children (Wang et al., 2012; Wu et al., 2012). The fourth study showed a weak correlation between VA and FD and central GCL+ thickness among children born EPT. Recently Bowl et al. (2016) showed that a subgroup of preterm born children (both with and without ROP) with an abnormal relation between foveal layer thicknesses at FC had reduced visual function as measured with microperimetry but not with VA. Molnar, Andréasson, Larsson, Åkerblom and Holmström (2017) measured the rod and cone function with full-field electroretinography in 52 children born EPT (from the Uppsala cohort in study 3) and identified reduced rod and cone function but without association to GA or ROP. Sjöstrand, Rosén, Nilsson and Popovic (2017) observed changes within the inner retinal layers of the fovea which may be of importance to explain the decreased central retinal function in preterms.

The increased GCL+ thickness seen in association to a preterm birth should be seen as a sign of an inhibited maturation and not as a sign of a truly healthy and thick GCL that is of any functional advantage.

The third study revealed thinner retina in the inner circle in children born EPT with a history of severe IVH that might be a result of ganglion cell loss and the fourth study revealed that these children actually has reduced total GCL+ thickness. Since there were only 12 eyes with severe IVH further studies are needed and visual field examination or magnetic resonance imaging tractography on these children could confirm the hypothesis of reduced GCL+ due to retrograde trans-synaptic degeneration.

CONCLUSION

The HRT3 and Stratus OCT showed no significant difference regarding the retinal thickness measurements between examiners or occasions. However, the measurements with the HRT3 had lower repeatability and reproducibility compared with the Stratus OCT and both examiners found Stratus OCT more user friendly both for the patients and the examiner. Therefore, the OCT seemed suitable for the examination of rather young children in the following studies, see figure 8. From the studies of 6.5 year old children born extremely preterm, the conclusions are that preterm birth before GA of 27 weeks commonly leads to permanent alterations of the foveal anatomy expressed as reduced FD and incomplete extrusion of the IRL. Due to this incomplete extrusion of IRL the macular thickness and the GCL+ are increased at the FC. Severe IVH is associated with reduced total GCL+ thickness and might be caused by trans-synaptic degeneration of the retinal ganglion cells. The outer retinal layers at the fovea generally develop well even though deviations of the ONL can be seen in children born EPT. The structural deviations, in the IRL, seen in prematurely born children seem to have little impact on visual acuity even though a weak correlation between FD and central GCL+ thickness and VA were found. The FD seems to be a good parameter to evaluate the maturity of the fovea since it is not biased of the thickness at FWM.

Figure 8. A girl gets her macula examined with Cirrus SD-OCT by me. Picture approved for publication by the child and both her parents.

7 ACKNOWLEDGEMENTS

I wish to express my warm gratitude to:

My main supervisor and co-author Maria Nilsson Senior Lecturer, PhD. Thank you for your encouragement, wise advice, support, patience and for always being available when I needed.

My associate supervisors and co-authors, Professor Lene Martin and Associate Professor Kerstin Hellgren, M.D., PhD, for your valuable knowledge, help and support.

My co-author and mentor, Associate Professor Leif Tallstedt, for your support and for always being friendly. It was a pleasure working with you.

My co-authors, Anna Molnar, M.D., PhD, Associate Professor Eva Larsson and Professor Gerd Holmström. It was a pleasure working with you.

My co-authors, Abinaya Venkataraman, PhD and Alberto Domínguez-Vicent PhD. Thank you for your support and for making a custom-made Matlab program.

Professor Emeritus Johan Sjöstrand and Zoran Popovic, PhD, Senior Research Engineer for all your help, enthusiasm and for sharing your knowledge.

My colleagues at the Unit of Optometry: Rune Brautaset PhD, Marika Wahlberg Ramsay PhD, Jaana Johansson, Kerstin Lutteman, Annika Botes, Susanne Glimne PhD, Elin Bergling, Marie Brenning, Petra Frehr Alstig and Marguerite Tjärnberg. It is a pleasure working with you! A special thanks to Lovisa Pettersson for your fine illustrations and my "roommate" Anna Lindskoog Pettersson for always supporting and encouraging me. Last but not least a big thank you to Ulrika Birkeldh, your help, support, encouragement and our conversations and discussions have been invaluable to me. We have struggled with our thesis side by side and we did well!

I am grateful to have had the opportunity to work with Monica Ferrato Sandén, Sara Björling, Christina Åkerstedt, Ulla Bremö, Sara De Lima, Fredrik Källmark PhD, Associate Professor Tony Pansell, Ulrika Sverkersten PhD, Alba Lucia Törnquist PhD, Sten Lutteman, and Inga-Lill Thunholm-Henriksson.

My colleagues at Stockholms Ögonklinik. It is a pleasure working with you!

My friends, you are wonderful! Thank you for making me laugh when I needed it the most and all our pleasant talks.

My parents Leif and Britt-Marie, for always believing in me and encouraging me in my work, studies and life choices. Thank you for your endless love and support.

My brother Samuel, his wife Lina and their children Inez, Henry and Stig, my brother Jonatan, his wife Sofia and their children Tove and Hjalmar for always being there with love and support. You are wonderful and I thank you for being a part of my life.

My children Iris and Emmy. I love you to the moon and back, you are the stars and sunshines of my life.

My husband Joakim, for your endless love and support. I love you to infinity and beyond, forever and ever.

8 REFERENCES

Ashton, N. (1970). Retinal angiogenesis in the human embryo. *Br Med Bull, 26*(2), 103-106.

Austeng, D., Källen, K. B., Ewald, U. W., Jakobsson, P. G., & Holmström, G. E. (2009). Incidence of retinopathy of prematurity in infants born before 27 weeks' gestation in Sweden. *Arch Ophthalmol, 127*(10), 1315-1319.

Barrio-Barrio, J., Noval, S., Galdós, M., Ruiz-Canela, M., Bonet, E., Capote, M., & Lopez, M. (2013). Multicenter Spanish study of spectral-domain optical coherence tomography in normal children. *Acta Ophthalmol, 91*(1), 56-63.

Brautaset, R., Birkeldh, U., Rosén, R., Ramsay, M. W., & Nilsson, M. (2014). Reproducibility of disc and macula optical coherence tomography using the Canon OCT-HS100 as compared with the Zeiss Cirrus HD-OCT. *Eur J Ophthalmol, 24*(5), 722-727.

Brautaset, R. L., Rosén, R., Cerviño, A., Miller, W. L., Bergmanson, J., & Nilsson, M. (2015). Comparison of Macular Thickness in Patients with Keratoconus and Control Subjects Using the Cirrus HD-OCT. *Biomed Res Int,* 2015;2015:832863.

Brown, N. P., Koretz, J. F., & Bron, A. J. (1999). The development and maintenance of emmetropia. *Eye (Lond), 13*(1), 83-92.

Bowl, W., Stieger, K., Bokun, M., Schweinfurth, S., Holve, K., Andrassi-Darida, M., & Lorenz, B. (2016). OCT-Based Macular Structure-Function Correlation in Dependence on Birth Weight and Gestational Age-the Giessen Long-Term ROP Study. *Invest Ophthalmol Vis Sci, 57*(9), 235-241.

Chan-Ling, T., Gock, B., & Stone, J. (1995). The effect of oxygen on vasoformative cell division. Evidence that 'physiological hypoxia' is the stimulus for normal retinal vasculogenesis. *Invest Ophthalmol Vis Sci, 36*(7), 1201-1214.

Chen, J., & Smith, L. E. (2007). Retinopathy of prematurity. *Angiogenesi, 10*(2), 133-140.

Curcio, C. A., & Allen, K. A. (1990). Topography of ganglion cells in human retina. *J Comp Neurol, 300*(1), 5-25.

Curcio, C. A., Sloan, K. R., Kalina, R. E., & Hendrickson, A. E. (1990). Human photoreceptor topography. *J Comp Neurol, 292*(4), 497-523.

De Moraes, C. G. (2013). Anatomy of the visual pathways. *J Glaucoma, 22*(5), 2-7.

Dubis, A. M., Costakos, D. M., Subramaniam, C. D., Godara, P., Wirostko, W. J., Carroll, J., & Provis, J. M. (2012). Evaluation of normal human foveal development using optical coherence tomography and histologic examination. *Arch Ophthalmol, 130*(10), 1291-300.

Early Treatment for Retinopathy of Prematurity Cooperative Group. (2003). Revised indications for the treatment of retinopathy of prematurity: results of the early treatment for retinopathy of prematurity randomized trial. *Arch Ophthalmol, 121*(12), 1684-1694.

Falavarjani, K. G., Iafe, N. A., Velez, F. G., Schwartz, S. D., Sadda, S. R., Sarraf, D., & Tsui, I. (2017). Optical coherence tomography angiography of the fovea in children born preterm. *Retina, 37*(12), 2289-2294.

Fellman, V., Hellström-Westas, L., Norman, M., Westgren, M., Källén, K., Lagercrantz, H., … Wennergren, M. (2009). One-year survival of extremely preterm infants after active perinatal care in Sweden. *JAMA, 301*(21), 2225-2233.

Fujimoto, J., & Swanson, E. (2016). The Development, Commercialization, and Impact of Optical Coherence Tomography. *Invest Ophthalmol Vis Sci, 57*(9), 1-13.

Gabriele, M. L., Wollstein, G., Ishikawa, H., Kagemann, L., Xu, J., Folio, L. S., & Schuman, J. S. (2011). Optical coherence tomography: history, current status, and laboratory work. *Invest Ophthalmol Vis Sci, 52*(5), 2425-2436.

Gordon, R. A., & Donzis, P. B. (1985). Refractive development of the human eye. *Arch Ophthalmol, 103*(6), 785-789.

Hansen J. T. (2010). Netter's anatomy coloring book. (1st ed). Philadelphia: Saunders Elsevier.

Hardin, J. S., Taibbi, G., Nelson, S. C., Chao, D., & Vizzeri, G. (2015). Factors Affecting Cirrus-HD OCT Optic Disc Scan Quality: A Review with Case Examples. J Ophthalmol. 2015;2015:746150.

Haugen, O. H, Nepstad, L., Standal, O. A., Elgen, I., & Markestad, T. (2012). Visual function in 6 to 7 year-old children born extremely preterm: a population-based study. *Acta Ophthalmol, 90*(5), 422-427.

Hellgren, K., Hellström, A., & Martin, L. (2009). Visual fields and optic disc morphology in very low birthweight adolescents examined with magnetic resonance imaging of the brain. *Acta Ophthalmol, 87*(8), 843-848

Hellgren, K. M., Tornqvist, K., Jakobsson, P. G., Lundgren, P., Carlsson, B., Källén, K., … Holmström, G. (2016). Ophthalmologic Outcome of Extremely Preterm Infants at 6.5 Years of Age: Extremely Preterm Infants in Sweden Study (EXPRESS). *JAMA Ophthalmol.*

Hellström, A., Smith, L. E., & Dammann, O. (2013). Retinopathy of prematurity. *Lancet, 382*(9902), 1445-1457.

Hendrickson, A. (2016). Development of Retinal Layers in Prenatal Human Retina. *Am J Ophthalmol, 161*, 29-35.

Hendrickson, A., Possin, D., Vajzovic, L., & Toth, C. A. (2012). Histologic development of the human fovea from midgestation to maturity. *Am J Ophthalmol, 154*(5), 767-778.

Hendrickson, A. E., & Yuodelis, C. (1984). The morphological development of the human fovea. *Ophthalmology, 91*(6), 603-612.

Hendrickson, A. E. (1994). Primate foveal development: a microcosm of current questions in neurobiology. *Invest Ophthalmol Vis Sci, 35*(8), 3129-3133.

Hintz, S. R., Kendrick, D. E., Vohr, B. R., Kenneth Poole, W., Higgins, R. D., & Nichd Neonatal Research Network. (2006). Gender differences in neurodevelopmental outcomes among extremely preterm, extremely-low-birthweight infants. *Acta Paediatr, 95*(10), 1239-1248.

Hirasawa, K., Shoji, N., Yoshii, Y., & Haraguchi, S. (2014). Determination of axial length requiring adjustment of measured circumpapillary retinal nerve fiber layer thickness for ocular magnification. *PLoS One, 9*(9):e107553.

Holmström, G., el Azazi, M., & Kugelberg, U. (1999). Ophthalmological follow up of preterm infants: a population based, prospective study of visual acuity and strabismus. *Br J Ophthalmol, 83*(2), 143-150.

Holmström, G., Hellström, A., Jakobsson, P., Lundgren, P., Tornqvist, K., & Wallin, A. (2016). Five years of treatment for retinopathy of prematurity in Sweden: results from SWEDROP, a national quality register. *Br J Ophthalmol, 100*(12), 1656-1661.

Horton, J. C., & Hoyt W. F. (1991). The Representation of the Visual Field in Human Striate Cortex. A Revision of the Classic Holmes Map. *Arch Ophthalmol, 109*(6), 816-824.

Huang, D., Swanson, E. A., Lin, C. P., Schuman, J. S., Stinson. W. G., Chang, W., … Puliafito, C. A. (1991). Optical coherence tomography. *Science, 254*(5035), 1178-1181.

Hughes, S., Yang, H., & Chan-Ling, T. (2000). Vascularization of the human foetal retina: roles of vasculogenesis and angiogenesis. *Invest Ophthalmol Vis Sci, 41*(5), 1217-1228.

International Committee for the Classification of Retinopathy of Prematurity. (2005). The International Classification of Retinopathy of Prematurity revisited. *Arch Ophthalmol,* 123(7), 991-999.

Jacobson, L., Hellström, A., & Flodmark, O. (1997). Large cups in normal-sized optic discs: a variant of optic nerve hypoplasia in children with periventricular leukomalacia. *Arch Ophthalmol, 115*(10), 1263-9.

Jacobson, L. K., & Dutton, G. N. (2000). Periventricular leukomalacia: an important cause of visual and ocular motility dysfunction in children. Surv *Ophthalmol, 45*(1), 1-13. Review.

Jacobson, L., Flodmark, O., & Martin, L. (2006). Visual field defects in prematurely born patients with white matter damage of immaturity: a multiple-case study. *Acta Ophthalmol Scand, 84*(3), 357–362.

Jaffe, G. J, & Caprioli, J. (2004). Optical coherence tomography to detect and manage retinal disease and glaucoma. *Am J Ophthalmol, 137*(1), 156-169.

Kolb, H. (2007). Midget pathways of the primate retina underlie resolution and red green color opponency. In H. Kolb, E. Fernandez, & R. Nelson (Eds.), *Webvision: The Organization of the Retina and Visual System.* Salt Lake City (UT): University of Utah Health Sciences Center; 1995-..

Larsson, E. K., Rydberg, A. C., & Holmström, G. E. (2003). A population-based study of the refractive outcome in 10-year-old preterm and full-term children. *Arch Ophthalmol, 121*(10), 1430-1436.

Lavinsky, F., & Lavinsky, D. (2016). Novel perspectives on swept-source optical coherence tomography. *Int J Retina Vitreous*, 2:25.

Lee, H., Purohit, R., Patel, A., Papageorgiou, E., Sheth, V., Maconachie, G., … Gottlob I. (2015). In vivo foveal development using optical coherence tomography. *Invest Ophthalmol Vis Sci, 56*(8), 4537-45.

Lee, Y. S., Chang, S. H. L., Wu, S. C., See, L. C., Chang, S. H., Yang, M. L., & Wu, W. C. (2018). The inner retinal structures of the eyes of children with a history of retinopathy of prematurity. *Eye, 32*(1), 104-112.

Lennartsson, F., Nilsson, M., Flodmark, O., & Jacobson, L. (2014). Damage to the immature optic radiation causes severe reduction of the retinal nerve fibre layer, resulting in predictable visual field defects. *Invest Ophthalmol Vis Sci, 55*(12), 8278-8288.

Lennartsson, F., Nilsson, M., Flodmark, O., Jacobson, L., & Larsson, J. (2018). Injuries to the Immature Optic Radiation Show Correlated Thinning of the Macular Ganglion Cell Layer. *Front Neurol.* 7;9:321.

Lujan, B. J., Roorda, A., Knighton, R. W., & Carroll, J. (2011). Revealing Henle's fibre layer using spectral domain optical coherence tomography. *Invest Ophthalmol Vis Sci, 52*(3), 1486-1492.

Maldonado, R. S., O'Connell, R. V., Sarin, N., Freedman, S. F., Wallace, D. K., Cotton, C. M., … Toth, C. A. (2011). Dynamics of human foveal development after premature birth. *Ophthalmology, 118*(12), 2315-2325.

Mann, I. (1964). *The development of the human eye* (3d ed.). New York,: Grune & Stratton.

Marmor, M. F., Choi, S. S., Zawadzki, R. J., & Werner, J. S. (2008). Visual insignificance of the foveal pit: reassessment of foveal hypoplasia as fovea plana. *Arch Ophthalmol, 126*(7), 907-913.

Maslin, J., Mansouri, K., & Dorairaj, S. (2015). HRT for the Diagnosis and Detection of Glaucoma Progression. *Open Ophthalmol J, 15*(9), 58–67.

McFadzean, R., Brosnahan, D., Hadley, D., & Mutlukan, E.(1994). Representation of the visual field in the occipital striate cortex. *Br J Ophthalmol, 78*(3), 185-190.

Mintz-Hittner, H. A., Knight-Nanan, D. M., Satriano, D. R., & Kretzer, F. L. (1999). A small foveal avascular zone may be an historic mark of prematurity. *Ophthalmology, 106*(7), 1409-1413.

Molnar, A. E. C., Andréasson, S. O., Larsson, E. K. B., Åkerblom, H. M., & Holmström, G. E. (2017). Reduction of Rod and Cone Function in 6.5-Year-Old Children Born Extremely Preterm. *JAMA Ophthalmol, 135*(8), 854-861.

Nilsson, M., Hellström, A., & Jacobson, L. (2016). Retinal Sequelae in Adults Treated With Cryotherapy for Retinopathy of Prematurity. *Invest Ophthalmol Vis Sci, 57*(9), 550-555.

O'Rahilly, R. (1975). The prenatal development of the human eye. *Exp Eye Res, 21*(2), 93-112.

Otani, T., Yamaguchi, Y., & Kishi, S. (2011). Improved visualization of Henle fibre layer by changing the measurement beam angle on optical coherence tomography. *Retina, 31*(3), 497-501.

Papile, L. A., Burstein, J., Burstein, R., & Koffler, H. (1978). Incidence and evolution of subependymal and intraventricular hemorrhage: a study of infants with birth weights less than 1,500 gm. *J Pediatr, 92*(4), 529-534.

Pierro, L., Giatsidis, S. M., Mantovani, E., & Gagliardi, M. (2010). Macular thickness interoperator and intraoperator reproducibility in healthy eyes using 7 optical coherence tomography instruments. *Am J Ophthalmol, 150*(2), 199-204.

Polyak, S. (1949). Retinal structure and colour vision. *Doc Ophthalmol, 3*(1), 24-56.

Provis, J. M., Billson, F. A., & Russell, P. (1983). Ganglion cell topography in human foetal retinae. *Invest Ophthalmol Vis Sci, 24*(9), 1316-1320.

Provis, J. M., Leech, J., Diaz, C. M., Penfold, P. L., Stone, J., & Keshet, E. (1997). Development of the human retinal vasculature: cellular relations and VEGF expression. *Exp Eye Re, 65*(4), 555-568.

Provis, J. M., van Driel, D., Billson, F. A., & Russell, P. (1985). Human foetal optic nerve: overproduction and elimination of retinal axons during development. *J Comp Neurol, 238*(1), 92-100.

Provis, J. M., & Hendrickson, A. E. (2008). The foveal avascular region of developing human retina. *Arch Ophthalmol, 126*(4), 507-511.

Rahi, J. S., & Cable, N; British Childhood Visual Impairment Study Group. (2003). Severe visual impairment and blindness in children in the UK. *Lancet, 362*(9393), 1359-1365.

Retina Module, Premium Edition Heidelberg retina Tomograph3, Operating Manual 19944-E01, Software Version 2.0. December 2006, Heidelberg Engineering GmbH

Rosén, R., Sjöstrand, J., Nilsson, M., & Hellgren, K. (2015). A methodological approach for evaluation of foveal immaturity after extremely preterm birth. *Ophthalmic Physiol Opt, 35(4)*, 433-441.

Sankar, M. J., Sankar, J., & Chandra, P. (2018). Anti-vascular endothelial growth factor (VEGF) drugs for treatment of retinopathy of prematurity. *Cochrane Database Syst Rev*, 8;1: CD009734.

Schraermeyer, U., & Heimann, K. (1999). Current understanding on the role of retinal pigment epithelium and its pigmentation. *Pigment Cell Res, 12*(4), 219-236.

Serenius, F., Ewald, U., Farooqi, A., Fellman, V., Hafström, M., Hellgren, K.,… Extremely Preterm infants in Sweden Study Group. (2016). Neurodevelopmental outcomes among extremely preterm infants 6.5 years after active perinatal care in Sweden. *JAMA Pediatrics, 170*(10), 954-963.

Sjöstrand, J., Olsson, V., Popovic, Z., & Conradi, N. (1999). Quantitative estimations of foveal and extra-foveal retinal circuitry in humans. *Vision Res, 39*(18), 2987-2998.

Sjöstrand, J., & Popovic, C. (2013). A time-line model of developmental events within the human fovea based on imaging and histology data. *Acta Ophthalmologica, 91*: 252.

Sjöstrand, J., Rosén, R., Nilsson, M., & Popovic, Z. (2017). Arrested Foveal Development in Preterm Eyes: Thickening of the Outer Nuclear Layer and Structural Redistribution Within the Fovea. *Invest Ophthalmol Vis Sci, 58*(12), 4948-4958.

Socialstyrelsen. (2018). Statistik om graviditeter, förlossningar och nyfödda barn 2016. http://www.socialstyrelsen.se/publikationer2018/2018-1-6.

Spaide, R. F., & Curcio, C. A. (2011). Anatomical correlates to the bands seen in the outer retina by optical coherence tomography: literature review and model. *Retina, 31*(8), 1609-1619.

Swanson, E. A., Izatt, J. A., Hee, M. R., Huang, D., Lin, C. P., Schuman, J. S., … Fujimoto, J. G. (1993). In vivo retinal imaging by optical coherence tomography. *Opt Lett, 18*(21), 1864-1866.

The Committee for the Classification of Retinopathy of Prematurity. (1984). An international classification of retinopathy of prematurity. *Arch Ophthalmol, 102*(8), 1130-1134.

The EXPRESS Group. (2010). Incidence of and risk factors for neonatal morbidity after active perinatal care: extremely preterm infants study in Sweden (EXPRESS). *Acta Paediatr, 99*(7), 978-992.

Thomas, M. G., Kumar, A., Mohammad, S., Proudlock, F. A., Engle, E. C., Andrews, C., … Gottlob, I. (2011). Structural grading of foveal hypoplasia using spectral-domain optical coherence tomography a predictor of visual acuity? *Ophthalmology, 118*(8), 1653-1660.

Tick, S., Rossant, F., Ghorbel, I., Gaudric, A., Sahel, J. A., Chaumet-Riffaud, P., & Paques, M. (2011). Foveal shape and structure in a normal population. *Invest Ophthalmol Vis Sci, 52*(8), 5105-5110.

Vajzovic, L., Hendrickson, A. E., O'Connell, R. V., Clark, L. A., Tran-Viet, D., Possin, D., … Toth, C. A. (2012). Maturation of the human fovea: correlation of spectral-domain optical coherence tomography findings with histology. *Am J Ophthalmol, 154*(5), 779-789.

Wagner-Schuman, M., Dubis, A., Nordgren, R., Lei, Y., Odell, D., Chiao, H., … & Carroll, J. (2011). Race- and Gender-Related Differences in Retinal Thickness and Foveal Pit Morphology. *Invest Ophthalmol Vis Sci, 52*(1), 625–634.

Wang, J., Spencer, R., Leffler, J. N., & Birch, E. E. (2012). Critical period for foveal fine structure in children with regressed retinopathy of prematurity. *Retina, 32*(2), 330-339.

Wu, W. C., Lin, R. I., Shih, C. P., Wang, N. K., Chen, Y. P., Chao, A. N., … Tsai, S. (2012). Visual acuity, optical components, and macular abnormalities in patients with a history of retinopathy of prematurity. *Ophthalmology, 119*(9), 1907-1916.

Wärntges, S., & Michelson, G. (2014). Detailed Illustration of the Visual Field Representation along the Visual Pathway to the Primary Visual Cortex: A Geographic Summary. *Ophthalmic Res, 51*(1), 37-41.

Yanni, S. E., Wang, J., Chan, M., Carroll, J., Farsiu, S., Leffler, J. N., … Birch, E. E. (2012). Foveal avascular zone and foveal pit formation after preterm birth. *Br J Ophthalmol, 96*(7), 961-966.

Yuodelis, C., & Hendrickson, A. A. (1986). Qualitative and quantitative analysis of the human fovea during development. *Vision Res, 26*(6), 847-855.